Sperm motility in mice with Oligo-astheno-teratozoospermia restored by in vivo injection and electroporation of naked mRNA

Charline Vilpreux[1], Guillaume Martinez[1,4], Magali Court[1], Florence Appaix[6], Jean-Luc Duteyrat[2], Maxime Henry[7], Julien Vollaire[7], Camille Ayad[3], Altan Yavz[3], Lisa De Macedo[1], Geneviève Chevalier[1], Emeline Lambert[1], Sekou Ahmed Conte[1], Elsa Giordani[1], Véronique Josserand[7], Jacques Brocard[2], Coutton Charles[1,4], Bernard Verrier[3], Pierre F. Ray[1,5], Corinne Loeuillet[1], Christophe Arnoult[1] and Jessica Escoffier[1*].

[1] Université Grenoble Alpes, Inserm U1209, CNRS UMR 5309, Team Genetic, Epigenetic and Therapies of infertility, Institute for Advanced Biosciences 38 000 Grenoble, France

[2] Université Claude Bernard Lyon 1, CNRS UAR3444, Inserm US8, ENS de Lyon, SFR Biosciences, Lyon 69007, France

[3]Université Claude Bernard Lyon 1 - Laboratoire de Biologie Tissulaire et d'Ingénierie Thérapeutique, UMR 5305, Université Lyon 1, CNRS, IBCP, Lyon, France

[4] UM de Génétique Chromosomique, Hôpital Couple-Enfant, CHU Grenoble Alpes, Grenoble, France.

[5] UM GI-DPI, CHU Grenoble Alpes, Grenoble, France.

[6] Université Grenoble Alpes, Inserm U1209, CNRS UMR 5309, plateforme microcell, Institute for Advanced Biosciences 38 000 Grenoble, France

[7] Université Grenoble Alpes, Inserm U1209, CNRS UMR 5309, plateforme Optimal, Institute for Advanced Biosciences 38 000 Grenoble, France

* To whom correspondence should be addressed: Jessica Escoffier, Team "Genetics, Epigenetics and Therapies of Infertility", Institute for Advanced Biosciences (IAB), INSERM 1209, CNRS UMR 5309 University Grenoble Alpes, Grenoble, FRANCE.
Contact:mail to jessica.escoffier@univ-grenoble-alpes.fr
tel: 33 (0)4 76 63 71 11

Ethics statement

All procedures involving animals were performed in line with the French guidelines for the use of live animals in scientific investigations. The study protocol was approved by the local ethics committee (ComEth Grenoble #318) and received governmental authorization (ministerial agreement #38109-2022072716142778).

Abstract

Oligo-astheno-teratozoospermia (OAT), a recurent cause of male infertility, is the most frequent disorder of spermatogenesis with a probable genetic cause. Patients and mice bearing mutations in the *ARMC2* gene have a decreased sperm concentration, and individual sperm show multiple morphological defects and a lack of motility – a canonical OAT phenotype. Intra Cellular Sperm Injection (ICSI) is required to treat such a condition but it has limited efficacy and was associated with a small increase in birth defects. Consequently, new targeted treatments are needed to restore spermatogenesis. Here, a combination of *in vivo* injection and electroporation of capped and poly-A-tailed naked mRNA is tested as a strategy to treat *ARMC2*-related infertility in mouse. mRNAs coding for several reporter genes are tested and the efficiency and the kinetic of expression are assessed using *in vivo* and *in vitro* 2D and 3D imaging experiments. We show that mRNA-coded reporter proteins are detected for up to 3 weeks mostly in germ cells, making the use of mRNA possible to treat infertility. We compare these results with those obtained with a more conventional DNA plasmid vector. In contrast, the use of the non-integrative plasmid Enhanced Episomal Vector (EEV) shows low and transient expression in spermatogenic cells. Consequently, injection and electroporation of naked mRNA-*Armc2* into the testes of *Armc2*-deficient males were performed and we show the presence of normal and motile sperm in the epididymis. This study shows for the first time that mRNA-*Armc2* efficiently restores spermatogenesis and opens new paths for male infertility treatment.

Key words: Sperm cells, infertility, protein therapy, mRNA, EEV, *In Vivo* Microinjection and Electroporation, *in vivo* imaging, Whole Testis Optical clearing, light sheet microscopy.

Introduction

Worldwide, 10-15% of couples (or 70 million) face infertility [1]. Infertility is thus a major public health issue presenting significant medical, scientific and economic challenges (a multibillion € annual market) [2]. A significant proportion of infertility is due to altered gametogenesis, where the sperm and eggs produced are incompatible with fertilization and/or embryonic development. Approximately 40% of cases of infertility involve a male factor, either exclusively, or associated with a female deficiency.

Male gametogenesis, or spermatogenesis, is a highly complex physiological process which can be split into three successive steps: proliferation (mitosis of spermatogonia), reduction of the number of chromosomes (meiosis of spermatocytes), and spermatid differentiation (spermiogenesis). The whole process involves several thousands of genes, of which a large part are expressed almost exclusively in the testes [3]. Because of this multiplicity of genes, spermatogenesis is strongly affected by genetic factors [3], with most severe disorders likely to be of genetic origin.

For patients with severe infertility, only assisted reproductive technologies (ARTs) – such as Intra Cytoplasmic Sperm Injection (ICSI) – can efficiently overcome the problems faced. However, there are some concerns surrounding the risks associated with this technique; statistical analyses of birth records has shown a real risk of birth defects associated with ICSI [4]. To overcome these drawbacks, a number of experimental strategies have been proposed to bypass ARTs and restore spermatogenesis, including gene therapy [5-8].

Gene therapy consists of introducing a DNA sequence into the genome to compensate for a defective gene. It can thus rescue production of a missing protein, and is now widely applied both in research and for the treatment of human diseases. Given the genetic basis of male infertility, the first strategy tested to overcome spermatogenic failure associated with monogenic diseases was delivery of an intact gene to deficient germ cells. Gene therapy works efficiently in germ cells, and numerous publications have shown that conventional plasmids can be transferred into spermatogonia in several species with a high success rate, allowing their transcription in all cells of the germinal lineage [5-8]. Most experiments were performed in mouse models, delivering DNA constructs into living mouse germ cells by testis electroporation after microinjection of a DNA-containing solution into the seminiferous

tubules. Using this method, it was possible to rescue meiosis and fertility in mouse models of infertility [5, 8]. However, the genetic changes induced are transmitted to any descendants. Consequently, gene therapy cannot be used to treat infertility in humans, as for both ethical reasons and to avoid any eugenic deviations, transmissible changes are illegal in humans in most countries. Moreover, genetic modification of germ cell lines presents multiple biological risks, including that of inducing cancer [9, 10]. Gene therapies have thus raised both ethical controversy and long-term safety issues.

For these reasons, we decided to test an alternative strategy to DNA transfection based on the use of naked mRNA. Thanks to this small change, there should be no risk of genomic insertion, and thus there is no question of heritable alterations. The first part of this study presents a complete characterization of the protein expression patterns obtained following transfection of naked mRNA coding for reporter genes into the testes of mice.

Among infertility disorders, oligo-astheno-teratozoospermia (OAT) is the most frequent; it is likely to be of genetic origin. Spermatocytograms for OAT patients show a decrease in sperm concentration, multiple morphological defects and defective motility. Because of these combined defects, patients are infertile and can only conceive by ICSI. The aim of this work was 1/ to perform a full characterization of the efficiency of naked mRNA to express proteins, using reporter genes, and 2/ to apply the protocol to a preclinical mouse model of OAT. Patients and mice carrying mutations in the *ARMC2* gene present a canonical OAT phenotype and are completely infertile. The preclinical *Armc2* deficient (*Armc2* KO) mouse model is therefore a valuable model to assess whether *in vivo* injection of naked mRNA combined with electroporation can restore sperm spermatogenesis. We chose this model for several reasons: first, it is an easy model to implement. Armc2 KO mice are sterile and all sperm exhibit short, thick or coiled flagella [13]. As a result, 100% of sperm are completely immobile, thus it should be easy to determine the efficacy of the technique by measuring sperm motility with a CASA system. Second, the Armc2 gene codes for an 867-amino acid protein and this large size represents a challenge for expression in the testis following electroporation.

To determine the efficacy of naked mRNA transfection as a method to achieve protein expression in the testes, we assessed the level of transcription of reporter proteins after mRNA injection compared to the injection of a non-integrating plasmid, the Enhanced

Episomal Vector (EEV). EEV is a vector derived from Epstein-Barr virus, it includes an EBV Ori and the EBNA1 protein. It does not integrate or modify the host genome. Replication of this vector is synchronized with host cell division [11, 12].

In the present in vivo work, we injected and electroporated three distinct mRNAs coding for the reporter proteins green fluorescent protein (GFP), luciferase (Luc) and mCherry, and an EEV episome vector containing the sequences coding for both GFP and luciferase reporter proteins. We first characterized and validated the method of injection via the rete testis followed by electroporation in adult males. Next, we compared the kinetics and patterns of expression of the electroporated mRNAs and EEV by several methods, including whole testis imaging, in vivo bioluminescence imaging and tissue clearing.

Then we used a preclinical mouse model of OAT to test the mRNA transfection protocol, with the aim of restoring fertility. Three- and 5-weeks after injection and electroporation of *Armc2*-mRNA into the testes of *Armc2* KO mice, we identified normal motile sperm cells in the epididymis.

Materiel and methods

Animals

All procedures involving animals were performed in line with the French guidelines for the use of live animals in scientific investigations. The study protocol was approved by the local ethics committee (ComEth Grenoble #318) and received governmental authorization (ministerial agreement #38109-2022072716142778).

The animals used were B6D2 F1 hybrid (♀ C57BL/6JRj crossed with ♂ DBA/2, Janvier laboratories;france) adult male mice aged between 8 and 25 weeks, and the *Armc2* KO mouse strain obtained by CRISPR-Cas9, as described in Coutton et al. 2019. Experiments were carried out on wild type (WT) or *Armc2* KO adult male mice aged between 8 and 15 weeks.

Chemicals and reagents

Fast Green (FG) (F7258 – 25 g), phosphate buffered saline (PBS, D853 7- 500 mL), hematoxylin (GH5316 – 500 mL), eosin (HT110216 – 500 mL), terbutanol (471712 – 100 mL), Histodenz (D2158 – 100 g), sorbitol (S1876 – 100 g) and urea (U5128 – 500 g) were

purchased from Sigma Aldrich (Saint Louis, MI, USA). Schorr staining solution was obtained from Merck (XXX). Mfel HF (R35895) and RNase-free DNase I (M03035) were obtained from New England Biolabs (Ipswich, MA, USA). Paraformaldehyde (PFA, 15710) was obtained from Electron Microscopy Science (Hatfield, PA, USA). Ketamine and xylazine were obtained from Centravet (Dinan, France). Fluorescent i-particles NIRFiP-180 were obtained from Adjuvatis (Lyon, France). CleanCap AG, CleanCAp *EGFP*-mRNA and CleanCap *Luciferase*-mRNA were obtained from Tebubio (Le Perray en Yvelines, france).

Plasmids

All plasmids were amplified by bacterial transformation (E. coli, EC0112; Thermo Fisher, Waltham, MA, USA). After expansion, plasmids were purified with a NucleoBond Xtra Midi kit (740410-50; Macherey-Nagel, Düren, Germany). DNA pellets were solubilized in (DNAse- and RNAse-free) milliQ water.

Non-integrative episome EEV *CAGs-GFP-T2A-Luciferase*

The EEV *CAGs-GFP-T2A-Luciferase* (EEV604A-2) used for *in vivo* testis microinjection and electroporation was obtained from System Biosciences (Palo Alto, CA, USA). This episome contains the cDNA sequences of Green Fluorescent Protein (GFP) and luciferase, under the control of a CAGs promoter (supp Fig 1). After purification, the EEV *CAGs-GFP-T2A-Luciferase* plasmid concentration was adjusted to 9 µg μL^{-1}. Prior to injection, 3.3 µL of this plasmid solution was mixed with 1 µL 0.5% Fast Green and 5.7 µL sterile PBS to obtain a final EEV concentration of 3 µg μL^{-1}.

***mCherry* plasmid**

The was obtained from Dr. Conti's lab at UCSF. This plasmid contains the cDNA sequence of *mCherry* under the control of CMV and T7 promoters (supp Fig 1). After amplification and purification, the final plasmid concentration was adjusted to 9 µg μL^{-1}.

Plasmid EEV-*Armc2-GFP*

The EEV-*Armc2-GFP* plasmid used for *in vivo* testes microinjection and electroporation was obtained from Trilink (San Diego, USA). This non-integrative episome contains the cDNA sequences of *Armc2* and the Green Fluorescent Protein (GFP) genes under the control of a strong CAGs promoter (Fig 1 supplementary).

After amplification and purification, the final plasmid concentration was adjusted to 9 µg $µL^{-1}$. Prior to injection, 3.3 µL of this plasmid solution was mixed with 1 µL of 0.5% Fast Green and 5.7 µL of sterile PBS to obtain a final EEV concentration of 3 µg $µL^{-1}$.

Armc2-mRNA

Armc2-mRNA used for in vivo testes microinjection and electroporation was obtained from Trilink (San Diego, USA). The commercial *Armc2*-mRNA has an AG CleanCap, a poly A tail of 120 adenosines and 3 HA FLAG. The main challenge with mRNA-based therapies is mRNA stability. To improve mRNA stability in vivo and avoid its degradation by ribonucleases, optimization techniques were implemented. Thus, the used mRNA had codon optimization, a polyA tail and a CleanCap. To verify germ the efficiency of cell transfection, an *EGFP*-mRNA was injected together with the *Armc2*-mRNA. During the injection, the concentration of *EGFP*-mRNA and *Armc2*-mRNA were 300 ng $µL^{-1}$ each.

mcherry*-mRNA transcription *in vitro

The circular *mCherry* plasmid was linearized using the restriction enzyme MfeI HF at 37 °C for 1 h. The pm-*mCherry* was then extracted and purified with the DNA Clean and Concentrator-25 ™ kit (D4033; Zymo Research, Irvine, CA, USA). The pm-*mCherry* was subsequently transcribed in vitro using the T7-FlashScribe kit (C-ASF3507; Tebubio, Le Perray en Yvelines, France). The mRNA was capped with a clean cap (CleanCap AG, Tebubio), and a poly A tail (C-PAP5104H; Tebubio) was added before purification using the NucleoSpin RNA Clean Up kit (740948-50; Macherey-Nagel). Prior to injection, *mcherry*-mRNA was mixed with Fast Green to obtain a final concentration of 300 ng $µL^{-1}$ (0.05% FG, PBS).

Agarose gel electrophoresis of the Episomal Vector EEV and mRNA-mCherry

Before loading on a pre-stained (Gel Green) 1.5% agarose gel, the EEV-plasmid and mRNA were mixed with a loading dye (Promega Blue Orange G1904). An aliquot of each sample (500 ng) was loaded into each well and electrophoresis was performed for 30 min at 100 V at room temperature (RT). A DNA size marker (Gene ruler, Thermo Scientific, SM1331) was used to assess molecular weight. Gel images were acquired using a ChemiDoc XRS+ (BIORAD).

***In vivo* microinjection and electroporation of testes**

Electroporation was conducted as previously described [7]. Briefly, male mice B6D2, *Armc2* +/+ or *Armc2* -/-, depending the experimental conditions, were anesthetized with ketamine/xylazine solution (100mg μL^{-1} and 10 mg μL^{-1} respectively). The testes were pulled out of the abdominal cavity or scrotum. Under a binocular microscope and using microcapillaries pipettes (FemtoTip II ®, Eppendorf, Montesson, France), 10 µL DNA (3 µg μL^{-1} -0.05% FG) or mRNA (300 ng μL^{-1} -0.05% FG) was injected into the seminiferous tubules through the *rete testis* applying constant pressure (microinjector, Femto Jet 4i). Two series of 8 square electric pulses (25 V for 50 ms) were applied to the testis using tweezer-type electrodes linked to an electroporator (Gemini, BTX, Holliston, USA). The testes were then replaced in the abdominal cavity, and the abdominal wall and skin were sutured. For each animal, the left testis was injected and electroporated with the different nucleic acids (mRNA, EEV), whereas the right testis was injected with a control solution (PBS, 0.5% FG) as a control. Both testes were electroporated.

Flash Freezing and Fluorescence Analysis of testes

Depending on the experimental condition, 1-, 3- or 7-days post injection, the testes were collected and washed for 5 min in PBS. Then, they were embedded in Peel-A-Way Cryomolds filled with OCT (OCT Mounting media VWR BDH CHEMICALS). The samples were flash frozen in a 100% isopentane solution (Carlo ERBA), pre-cooled with liquid nitrogen. Once frozen, they were cut into 20-µm sections using a cryostat. The cryostat sections were then fixed with 4% PFA-PBS for 10 min at 4 °C and counterstained with 1.8 µM DAPI (nuclear stain) before observation using an Axioscan Z1 slide scanner or a confocal AxioObserver Z1 multiparameter microscope LSM710 NLO – LIVE7 – Confocor3 . The fluorescence of the different reporter proteins was detected using appropriate filters for DAPI, GFP, Texas Red (for mCherry), and Cy7 (for the Fluorescent i-particles NIRFiP-180).

Tissue collection and histological analysis

For histological analysis, treated and control B6D2 testes were fixed by immersion in 4% paraformaldehyde (PFA) for 14 h. They were then embedded in paraffin before cutting into 5-µm sections using a microtome (Leica biosystems). After deparaffination, the sections were stained with hematoxylin and eosin. Stained sections were digitized at ×20 magnification using an axioscan Z1-slide scanner (Zeiss, Germany). Spermatogenesis was assessed by measuring the area of seminiferous tubules (μm^2) and the cross

sections of round tubules (($n > 35$ tubules per testis section; n= 5 testis sections per condition). Statistical significance of differences was determined using a Student *t*-test.

Ex vivo Fluorescence Analysis

To analyze the expression of the reporter proteins GFP and mCherry in seminiferous tubules, whole testes were examined under an inverted microscope (Olympus, CKX53). Exogenous fluorescence was detected using filters for GFP and Texas Red.

Harris-Shorr sperm Analysis

Sperm cells were collected from the caudae epididymides of mice (Control, injected with EEV-*GFP*, *GFP*-mRNA, or *Armc2*-mRNA). They were allowed to swim for 10 min at 37 °C in 1 mL M2 media. Sperm cells were centrifuged at 500 x g, washed once with PBS, and fixed in PBS/4% paraformaldehyde for 1 min at RT. After washing with 1 mL acetate ammonia (100 mM), the sperm cell suspensions were spotted onto 0.1% poly L-lysine precoated slides (Thermo Scientific) and left to dry. Harris–Schorr staining was then performed according to the WHO protocol [14], and at least 100 sperm cells were analyzed per animal.

Whole Testis Optical clearing and 3D image reconstructions

<u>Optical clearing (adapted from uDISCO and Fast 3D clear protocols)</u>

Adult mice were euthanized by cervical dislocation and transcardial perfusion with 1X PBS (Sigma-Aldrich). The testes were extracted and fixed for two days at 4 °C in 4% PFA (Electron Microscopy Sciences). Samples were then washed with PBS for at least two days. Mouse testes were subsequently dehydrated in graded series of tert-butanol solutions (Sigma-Aldrich) at 35 °C as follows: 30% overnight (O/N), 50% for 24 h, 70% for 10 h, 80% O/N, 90% for 10 h, 96% O/N, and 100% for 10 h. The testes were cleared in clearing solution (96 % Histodenz,2% Sorbitol ,20 % Ure) for 2 days. Then, nuclei were stained with 3.6 µM DAPI (20% DMSO; 2% Triton, 1% BSA) for 2 days. Finally, the testes were then conserved in the clearing solution at 4°C until the microscopy observation. All these steps were carried out under agitation and protected from light.

<u>3D tissue Imaging</u>

The optically-cleared mouse testes were imaged on a lightsheet fluorescence microscope (Blaze, Miltenyi Biotec, Germany), using a 4x NA 0.35 MI PLAN objective protected by a dipping cap for organic solvents, with an overall working distance of 15 mm. Acquisitions on the horizontal plane were obtained with a fixed lightsheet thickness of 3.9 µm at both 488 nm and 561 nm with no overlap between horizontal planes. Voxel resolution x = 1.21; y = 1.21; z = 2 µm. 3D reconstructions were created using Imaris software (Oxford Instruments plc, Tubney Woods, Abingdon, Oxon OX13 5QX, UK).

Cellular image analysis

The optically-cleared mouse testes were imaged using a 'ConfoBright' system which is a unique adaptive confocal microscope (Nikon A1R MP, Nikon Europe B.V., The Netherlands) equipped with a deformable mirror module (AOS-micro, AlpAO, Montbonnot, France) for the correction of geometrical aberrations. Indeed, the deep confocal imaging of the cleared 3D sample requires long distance objectives and immersion media of different refractive index, resulting in optical aberrations. Images were acquired using Adaptive Optics optimization with an apo LWD 40x/1.15 water immersion objective (WD 600 µm) and a 10x/0.45 objective. FIJI software was used to process and analyze images and Imaris software for the 3D reconstructions.

Bioluminescence imaging

In vivo Bioluminescence imaging was performed at several time points after *in vivo Luciferase* -mRNA or EEV-*GFP-luciferase* injection and electroporation (n = 5 mice per condition). Ten minutes before imaging, mice received an intraperitoneal injection of 150 µg g^{-1} of D-luciferin (Promega), and were then anesthetized (isoflurane 4% for induction and 1.5% for maintenance) before placing in the optical imaging system (IVIS Lumina III, PerkinElmer). *In vivo* bioluminescence signals were measured in selected regions of interest (injected testes) and were expressed as mean photons per second (mean ± SEM). Background bioluminescence was measured on images from control mice. When the *in vivo* bioluminescence signal was no longer detectable, testes were collected and immersed in a luciferin solution for a few minutes before performing *ex vivo* imaging to confirm the absence of signal.

Sperm motility

296 The cauda epididymis was dilacerated in 1 mL of M2 medium (Sigma-Aldrich, l'Isle d'Abeau,
297 France) and spermatozoa were allowed to swim out for 10 min at 37 °C. Motility of the
298 spermatozoa was evaluated with an Olympus microscope and Computer Aided Sperm
299 Analysis (CASA) (CEROS II apparatus; Hamilton Thorne).

300 **Western blot**

301 Western blotting was performed on HEK-293T cells (ATCC, Manassas, VA, USA) transfected
302 with EEV-*Armc2* or *Armc2*-mRNA. Cells were transfected using JetPrime (Polyplus,
303 101000027) for DNA and JetMessenger (Polyplus, 101000056) for mRNA vectors, both
304 according to the supplier's recommendations. After 48 h, the cells were washed with PBS
305 and scraped off before centrifuging at 4 °C, 1500 RPM for 5 min. The cell pellet was then
306 resuspended in lysis buffer (Thermo Scientific, 87787) supplemented with an EDTA-free
307 cocktail of protease inhibitors (Roche, 11836170001). The suspension was stirred at 4 °C for
308 2 h, and then centrifuged at 16,000 x g at 4 °C for 10 min. The protein content of the
309 supernatant was estimated (QuantiPro™ BCA Assay kit; Sigma-Aldrich QPBCA) before adding
310 5X Laemmli + 5% β-mercaptoethanol and heating at 95 °C for 10 min. For the Western blot,
311 30 µg of proteins were deposited on a ready-made Bis-Tris gel 12 % (ThermoFisher). After
312 transfer, the PVDF membrane was blocked with 5% milk in Tris-Buffered Saline solution
313 containing 0.1% Tween 20 (TTBS) before immunodetection. The anti HA antibody (Cat. No.
314 11867423001, Sigma Aldrich) was diluted in TTBS at 1/5000. After incubation with secondary
315 antibodies (AP136P, Sigma Aldrich, 1:10,000 in TTBS), binding was revealed with an
316 enhanced chemiluminescence detection kit (ECL plus, Amercontrol Biosciences). Membranes
317 were imaged on a ChemiDoc™ system (Bio-Rad).

318 **Immunofluorescence**

319 Immunofluorescence analysis of dissociated testicular cells was performed as follows. After
320 collection, the tunica albuginea was removed from the testes. Then the tissue was
321 mechanically digested with 18G needles. Once washed with PBS, the testicular cells were
322 placed in a dissociation medium (25 mL RPMI and 25 mg collagenase type V) for 20 min at
323 37 °C. After filtration (100 µM filter) and centrifugation (5 min at 200 x g) the pellets were
324 resuspended in PBS before centrifugation once again. The pellet was then fixed in 1 mL PFA
325 4% for 5 min. Then 10 mL of ammonium acetate (0.1 M) was added. Finally, 2 mL of medium
326 was spread on a slide. Testicular cells were permeabilized with 0.1% PBS-Triton X-100 for

20 min at room temperature. Slides were then blocked in 10% BSA with PBS-Tween 0.1% for 30 min before incubating overnight at 4 °C with primary antibodies anti-rabbit *ARMC2* (HPA053696, Sigma Aldrich, 1:50) and anti-guinea pig tubulin (AA345, Swiss Institute of Bioinformatics, 1:100) diluted in PBS-Tween 0.1% - 5% BSA. Slides were washed with PBS before incubating for 1 h with secondary antibodies (for tubulin: A-11073, Thermo Fischer Scientific, 1/500; for ARMC2: A-11036, Thermo Fischer Scientific, 1:1000). Samples were counterstained with DAPI and mounted with DAKO mounting media (Life Technology). Fluorescence images were acquired under a confocal microscope (Zeiss) fitted with a 63× oil immersion objective. Images were analyzed with ZEN lite software (Zeiss).

Statistical analyses

Statistical analyses were performed using SigmaPlot (version 10; Systat Software, Inc., San Jose, CA). To account for sample variability between animals, a paired t-test and Wilcoxon test were used. Data are displayed as mean ± SEM. P values of *≤0.05, **≤0.01, or ***≤0.001 were considered to represent statistically significant differences.

Results

1. ***In vivo* microinjection and electroporation of mouse testes**

Two routes have been described for microinjection of DNA into the testes: direct injection through the *tunica albuginea*, or injection into the lumen of the seminiferous tubules via the *rete testis*. We chose the *rete testis* route and evaluated the efficacy of the microinjection protocol, in particular as we wished to better characterize the diffusion of the injected solution in the volume of the testis, as we were unable to find any information on this parameter in the literature. The efficacy of microinjection *via rete testis* was assessed using fluorescent i-particles NIRFiP-180, and by measuring their diffusion in testis cross sections examined by microscopy 3 days post-injection (Fig 1). To avoid lesions due to overfilling, the injection was controlled by measuring the expansion of the staining of the peripheral seminiferous tubules during the injection. Injections were stopped when the testes were filled to 2/3 of their capacity (fig 1 A-B). In testis cross sections, the fluorescent i-particles NIRFiP-180 were heterogeneously distributed, and mainly observed in seminiferous tubules located in the peripheral region of the testes, with fewer particles present in the center of the testes (Fig 1 C-D). Moreover, no fluorescent i-particles NIRFiP-180 were visible in the

peritubular space. These results indicated that microinjection through the *rete testis* did not produce a homogenous distribution of the particles throughout the seminiferous tubules. Nevertheless, the seminiferous tubules remained intact, as no signal was observed in the peritubular space (Fig 1C-D).

Next, we assessed the overall safety of the *rete testis* microinjection and electroporation of mRNA and EEV into testes. The safety of the protocol was evaluated by comparing macroscopic and microscopic anatomies of control (injected with control solution, PBS, 0.05% FG), and treated testes (injected either with EEV-*GFP* (PBS, 0.05% FG) or *GFP*-mRNA (PBS, 0.05 % FG)). Three days post-injection, the testes were first observed under a binocular microscope to identify possible macroscopic degeneration of the seminiferous tubules (Fig 2A1 and 2B1). Degenerations appear as pearly white lesions at the surface of the testis as illustrated in Supp Fig 1 following over electroporation. With the protocol used, no such lesions were observed. Next, the testes were measured and weighted. No differences were observed between control and treated testes (Fig 2 A2, A3, B2, B3), Then, microscopic differences were sought by histological analysis of 5-µm sections (Fig 2C). No difference was observed between the control condition and EEV-*GFP* or *GFP*-mRNA on the full cross sections (Fig 2 C1, C2, C3). Next, we observed all the different testicular cells, including spermatogonia, spermatocytes, Sertoli cells, round spermatids and epidydimal sperm cells (Fig 2D1, D2, D3) in each condition. The layered structure of germ cells was respected in all cases. Analysis of the histological sections revealed no differences in the tubules area of the testes injected either with EEV-*GFP* or *GFP*-mRNA (Fig 2E). Finally, Harris-Shorr staining of the epididymal sperm cells showed no morphological defects (Fig 2F). Taken together, these results suggest that *in vivo* microinjection and electroporation of EEV or mRNA is safe.

2. Analysis of EEV-*GFP* and *GFP*-mRNA testicular expression by whole testis imaging

After validating the injection method, we compared the kinetics of GFP expression for mRNA and EEV. To do so, we injected and electroporated one testis of129 adult B6D2 mice with EEV-*GFP* and of 65 mice with *GFP*-mRNA. At 0, 1, 7, 15, 21-, 28-, 35- 42 and 49-days post-injection, the whole testes were observed under an inverted microscope. The exogenous fluorescence was directly visible at the surface of the testes when illuminated with light at the appropriate wavelength (Fig 3 and 4). These observations revealed no testicular lesions at any post-injection time (Fig 3.A1-H1 and 4A1-F1). In addition, both *GFP*-mRNA and EEV-

388 *GFP* induced GFP expression in the testes (Fig 3A2-H2 and 4A2-F2). It is worth noting that
389 both vectors induced GFP expression from the very first day. However, the durations of
390 expression were different. For EEV, GFP fluorescence was still observable on day 42 for 100%
391 of samples, and 56% of samples were positive on day 49, indicating that expression lasted
392 around 1.5 months (Fig 4G). In contrast, for mRNA, 100% of testes were labelled on day 21,
393 but none showed any fluorescence on day 28 (Fig 4G). Thus, EEV transfection allowed a
394 considerably longer duration of expression than mRNA. (Fig 3 and 4). In addition to
395 differences in duration of expression, the GFP expression patterns were clearly different:
396 mRNA produced a large, diffuse pattern, highlighting the shape of the seminiferous tubules;
397 EEV-*GFP* produced a punctiform pattern (Fig 3B and 4B.) These results suggest that *GFP*-
398 mRNA and EEV-*GFP* targeted different testicular cell types, or that there were differences in
399 terms of efficiency of transfection.

400 ***3.* Kinetics of EEV and mRNA expression assessed by *in vivo* imaging.**

401 To further assess and compare the kinetics of expression of the two vectors, we expressed
402 exogenous luciferase in the testis using EEV or mRNA and observed the level of luciferase by
403 *in vivo* bioluminescence imaging. For EEV, we took advantage of the fact that the EEV
404 plasmids contains the DNA sequence of the luciferase protein (CAGs-GFP-T2A-Luciferase) in
405 addition to the DNA sequence of the GFP fluorescent protein (Fig supp 2). For mRNA, we
406 injected commercial naked *luciferase*-mRNA into the *rete testis* according to the same
407 protocol as used for *GFP*-mRNA. For this set of experiments, we injected the EEV-*GFP-Luc*
408 and *luciferase*-mRNA into the testes of 6 adult mice on day 0. Importantly, we injected a
409 similar number of copies of mRNA and EEV. The testes were imaged *in vivo* to detect
410 bioluminescence expression, on day 1 and weekly until disappearance of the signal, no more
411 than 120 days post-injection (Fig 5). For EEV-*GFP-Luciferase*, the bioluminescence induced by
412 transfection was detected from day 1. After a rapid decrease in signal intensity over the first
413 3 weeks, a weak but constant signal remained detectable for 3 months, then faded away (Fig
414 5 A1-A2). For *Luciferase*-mRNA, expression was also detected from day 1. The
415 bioluminescence decreased gradually over 3 weeks, becoming undetectable thereafter (Fig
416 5B1-B2). These results are consistent with our previous results (Fig 3) and confirm that EEV
417 allows a longer expression of exogenous protein within the testis. Overall, our results
418 indicated stronger expression for mRNA than for EEV, but with expression decreasing rapidly

419 over-time, and almost no remaining signal after 3 weeks. In contrast, residual expression was
420 detectable for several months with EEV.

421 **4. Assessing testicular and cellular *GFP*-mRNA expression using whole testicle optical**
422 **clearing, light sheet microscopy, and 3D-microscopic reconstructions**

423 To better characterize the spatial distribution of *GFP*-mRNA expression in the testis, we
424 performed whole testicular optical clearing. On day 0, we injected and electroporated 6
425 testes with *GFP*-mRNA. On day 1, we harvested the testes, cleared them with a modified
426 optical clearing protocol (see Methods). After complete clearing (Fig 6 A), we observed the
427 testes under a light sheet microscope and performed 3D reconstruction (video 1, 2 and Fig 6
428 BC). From this 3D reconstruction, we determined the volume of testis stained with GFP. The
429 testis was sliced into 500 stacks, and the volume occupied by GFP staining was estimated by
430 measuring the GFP-positive area in each stack and multiplying it by the thickness of the stack
431 (10 µm). Measurements were possible only for the first 250 stacks due to optical problems
432 with the last 250 stacks. To overcome this problem, and acquire information for the whole
433 testis, the sample was turned by 180° and the measures repeated. A total GFP-stained
434 surface of 0.51 mm^3 and 0.23 mm^3 was determined for face 1 and face 2, respectively. The
435 corresponding total volume for the 250 stacks was measured as 60 mm^3, therefore 0.81%
436 and 0.24% of the testis volume was transfected for face 1 and face 2 respectively (Fig 6 BC).

437 **5. Assessing GFP cellular expression using whole testicle optical clearing and confocal**
438 **microscopy**

439 Because the GFP fluorescence patterns were different for the two nucleic vectors when
440 observed under the inverted microscope (Fig 3), we wondered whether the same cell types
441 were targeted in both cases. To address this question, the whole optical cleared testes from
442 EEV-*GFP* and *GFP*-mRNA-transfected mice were observed under a confocal microscope. The
443 different cell types were identified based on their positions within the seminiferous tubule,
444 their cellular shape and their nuclear morphology - revealed by nuclear staining. For
445 instance, Sertoli cells have an oval to elongated nucleus and the cytoplasm presents a
446 complex shape ("tombstone" pattern) along the basement membrane [15]. Round
447 spermatids have small, round and compact nuclei with a nucleole and are localized between
448 the spermatocytes and elongated spermatids [16]. For EEV-*GFP*, on day 1 post injection and

electroporation, a strong punctiform green fluorescence was visible inside the seminiferous tubules (Fig 7 A). Based on the different morphological criteria, this fluorescent signal was detected in spermatocytes, round spermatids and Sertoli cells (Fig 7 BC). On day 7, the GFP signal induced by EEV-*GFP* was reduced and only isolated signals in a few seminiferous tubules (1 per 11 tubules) were observed (Fig 7 D). These signals were associated only with Sertoli cells (Fig 7 E).

For the mRNA vector, on day 1 and day 7 post-injection and electroporation, an intense fluorescence was observed in all the germ cells in the seminiferous tubules (Fig 8). At the cellular level, this fluorescent signal was associated with Sertoli cells, spermatogonia, spermatocytes, round spermatids, elongated spermatids, and sperm cells to similar extents for both post-injection times (Fig 8 B, D). In contrast to what was observed with EEV on day 7, no reduction in the number of fluorescent seminiferous tubules was noted when using *GFP*-mRNA, with 8 out of 10 tubules stained (Fig 8C).

6. Expression of naked *mcherry*-mRNA in testis following electroporation

Heterologous expression is well known to depend on the protein studied, we therefore tested the same reporter proteins to compare the mRNA and EEV vectors in the experiments presented above. Apart from the bioluminescence experiments with luciferase, we compared only GFP protein expression. To validate and confirm the capacity of naked mRNA to safely express proteins in the testes after injection and electroporation, we further challenged the method with another reporter protein – mCherry. We injected homemade naked mRNA coding for mCherry into the testes (Fig supp 2BC). As previously with *GFP*-mRNA, no testicular lesions were observed (Fig supp 3 A1, B1, C1, D1, E1, F1). Assessment of the remanence of testicular expression of the mCherry fluorescent protein on days 0, 1, 7, 15 ,21 and 28 post- injections revealed a strong red fluorescence from day 1 that remained detectable 15 days post-injection (Fig supp3 B2, C2 and D2). At the cellular level, the fluorescent signal was detected in germ cells, including spermatogonia, spermatocytes, round spermatids, testicular sperm cells, and Sertoli cells on days 1 and 7 post-injection (Fig supp 4).

Finally, we compared the kinetics and levels of expression of the three different mRNA molecules, coding for mCherry, GFP and luciferase. By comparing the number of mice

expressing *mCherry*-mRNA, *GFP*-mRNA and *luciferase*-mRNA fluorescence/luminescence over 21 days, we observed first that expression was detectable for all mRNAs on day 1, and second that the duration of expression was slightly different for the individual mRNAs. For instance, on day 15, 100%, 80% and 60% of mice injected with *GFP*-mRNA, *mcherry*-mRNA, and mRNA-*luciferase*, respectively presented fluorescence/bioluminescence and on day 21 100% of mice expressed GFP, whereas no signal was observed for mCherry or Luciferase (Fig supp 5).

7. Endogenous expression of ARMC2 in germ cells

Before attempting to rescue expression, we felt it was important to better characterize Armc2 expression in healthy germ cells, and in particular to study the timing of expression. By IF, we determined when ARMC2 protein translation started during spermatogenesis. For these experiments, dissociated cells from testes were observed to detect the presence of ARMC2 on different spermatogenic cells. ARMC2 was present only in the flagellum of elongated spermatids (Fig 9A). The specificity of the signal was validated using testicular cells from Armc2 KO mice, where no signal was observed on all spermatogenic cells (Fig 9B). In WT cells, no evidence of ARMC2 was found in earlier germ cell types like spermatogonia or spermatocytes (data not shown). These results suggest that the ARMC2 protein is expressed late during spermatogenesis.

8. Co-injection of *Armc2*-mRNA and *eGFP*-mRNA followed by electroporation is safe and induces green fluorescence in the seminiferous tubules.

We next tested whether the injection and electroporation of two RNA molecules had any deleterious effects on testis anatomy and seminiferous tubule structure. We first verified the quality of *Armc2*-mRNA synthesis by transfecting HEK cells and performing Western blot (Fig supp 2). After this validation, we co-injected *Armc2*-mRNA and *eGFP*-mRNA into the left testes of mice, using the right testes as untreated controls. *eGFP*-mRNA was co-injected to verify and monitor transfection efficiency. The testes were observed under a binocular microscope at different times (3, 6, 10, 15, 21, 28 and 35 days) after electroporation to identify possible macroscopic degeneration of the seminiferous tubules. No morphological defects were observed in the testes co-injected with *Armc2*-mRNA and *eGFP*-mRNA. An example of control and injected testes from day 15 is presented in Fig 10 A1, B1. The testes

were also weighed at different times post-injection, and the weight ratios of injected testes to non-injected control testes were determined. For all time points, this ratio was close to 1 (Fig 10 C), confirming that the method and the mRNAs did not cause any injury at the organ level. Next, under blue light, the efficiency of the transfection was assessed by observing the GFP fluorescence at the surface of the testes. Obvious GFP fluorescence was observed on testes injected with *Armc2*-mRNA and *eGFP*-mRNA 2 weeks after injection (Fig 10 B2), indicating that the naked mRNA was successfully transfected into testicular cells and remained present up to 2 weeks after surgery.

9. Motile sperm cells detected in *Armc2* KO mice following *Armc2*-mRNA injection and electroporation into testes

We then assessed whether the injection of *Armc2*-mRNA into the testes in *Armc2* KO mice restored sperm cell motility. We examined motility of sperm cells present in the caudal part of the epididymis at different times post-injection (3 to 35 days post-injection). For each condition, between 3 and 5 KO mice were used.

The *Armc2* KO model used is known to produce sperm cells with short and irregular flagella that are therefore immotile on day 0. No motile sperm were observed on days 3, 6, 10, 15 or 28 after surgery (Fig 11 A). However, motile sperm cells were found in the epididymis of some *Armc2* KO mice at 21- and 35-days post-treatment (Fig 11 A). Indeed, 1 in 3 mice had motile sperm cells at 21 days post-surgery, rising to 3/5 mice at 35 days post-injection. Nevertheless, the number of motile sperm cells observed remained low: 4.5% after 21 days and 6.15% after 35 days post-injection (Fig 11 A). Videos showing sperm motility in different conditions are available in the online material associated with this article (Videos 3 to 6).

After verifying motility, we looked at the morphology of the spermatozoa present in the cauda epididymis. Six days after injection of *Armc2*-mRNA, the cells detected were mostly round cells and abnormal spermatozoa with a short or coiled flagellum measuring between 7 and 20 µm. The same cell types were observed at 3-, 10-, 15- and 28-days post-surgery.

In contrast, the motile sperm detected on days 21 and 35 had a normal morphology with a long flagellum (greater than 100 µm) and a hook-shaped head (Fig 11 B).

Discussion

The challenge of treating male infertility remains to be addressed. Current assisted reproduction techniques (ARTs) are unable to treat all patients, and alternative strategies need to be developed to meet the legitimate desire to be a father. The aim of this study was to evaluate the potential of naked mRNA as a means to induce expression of exogenous proteins in male germ cells in a preclinical adult mouse model. Based on previous studies using electroporation, we investigated whether the combination of the injection of naked mRNA and in *vivo* electroporation could lead to efficient protein expression in spermatogenic cells. We chose to first study the efficiency of capped and poly-A-tailed mRNA coding for reporter proteins and compared results to those obtained with a non-integrative enhanced episomal vector plasmid. No EEV plasmid has ever been tested in the context of infertility treatment before this study.

Using an adult mouse model, we optimized the micro-injection and electroporation method described by Michaelis et al [7]. We show that the microinjection through the *rete testis* did not provide a homogenous distribution of the particles throughout the seminiferous tubules. Nevertheless, the seminiferous tubules remained intact, with no signal detected in the peritubular space. The peripheral expression observed was not due to the close vicinity of cells to the electrodes, but rather to a peripheral dispersal of the injected solution, as shown by the distribution of the fluorescent i-particles NIRFiP-180. Our results also showed that the combination of injection and electroporation is safe when electric pulses are carefully controlled. Using such a protocol, we were able to induce the expression of 3 reporter proteins, GFP, mCherry and luciferase in the testis by mRNA injection/electroporation. Based on whole testes fluorescence and, for the first time, *in vivo* bioluminescence imaging of testes, we characterized the kinetics of mRNA expression. Expression was observed to decrease rapidly after electroporation, with the total duration ranging from 15 to 21 days, depending on the molecule being expressed. Using whole testicular optical clearing, the reporter proteins were synthetized from the injected mRNA in Sertoli cells, spermatogonia, spermatocytes, round spermatids, and spermatozoa from day 1, and were still detectable after 1 week.

When using the EEV vector, expression persisted for longer – up to 119 days – but with a lower yield of seminiferous tubule and cellular transfection. In particular, a lower level of

transfection of germ cells was observed than with the mRNA, and after 1 week, only Sertoli cells remained transfected.

These results suggest that although EEV expression lasted longer, mRNAs, by targeting more efficiently male germ cells and allowing higher transfection yields of seminiferous tubules, could be a more effective and potent tool to express exogenous proteins in germ cells. By expressing a missing protein in the case of male infertility due to monogenic causes, it could be possible to restore failed spermatogenesis and thus to treat infertility.

ARMC2 is expressed in late spermatogenesis stages

Dissociated WT testicular cells contained ARMC2 in the flagellum of spermatids. No *Armc2* expression was detected in earlier germ cell type lineages like spermatogonia. These results suggest that the ARMC2 protein is expressed late during spermatogenesis, which explains why motile sperm were only found in the cauda epididymis from 3 weeks after injection in our treated mice. Indeed, full spermiogenesis (from round cell to sperm) takes around 15 days [17], and the journey across the epididymis lasts around 8 days, making a total of 3 weeks. Our results also confirm those recently published by Lechtreck et al. [18] from their study of the role of ARMC2 in the Intra-Flagellar Transport (IFT) of radial spokes in *Chlamydomonas*. Proteins are supplied to the flagellum by IFT trains, with some proteins binding directly to IFT train subcomplexes. This is the case, for example, for tubulin, which binds to the N-terminal domains of the central IFT-B proteins IFT74 and IFT81 [19]. In other cases, protein binding is mediated by adapters. For example, the placement of the Outer Dynein Arms (ODA) requires an adapter protein ODA16 [20]. Lechtreck et al. [18] suggested that the transport of the radial spokes along the flagellum involves ARMC2 acting as an IFT adapter [18]. The presence of ARMC2 in the flagella of elongating spermatid supports this hypothesis.

Exogenous *Armc2*-mRNA expression rescued the motility of oligo-astheno-teratozoospermic sperm

This is the first demonstration that proteins can be expressed in the testis following electroporation with capped and poly-A-tailed mRNA.

Our objective was to develop a new targeted therapeutic approach for infertility associated with monogenic defects. In this preclinical study, we tested the ability of mRNA to restore

flagellar motility in a mouse model deficient for *Armc2* that displays an oligo-astheno-teratozoospermia .

Our results strongly suggest that the strategy is safe, as injection and electroporation of *Armc2*-mRNA or EEV-*Armc2* had no effect on testicular morphology or weight. More importantly, the technique was effective, with motile sperm cells found in *Armc2* KO epidydimal cauda 3 and 5 weeks after *Armc2*-mRNA injection. Naked mRNA injection/electroporation is therefore a promising method to treat infertility. In contrast, no motile spermatozoa were found after injection/electroporation of EEV-*Armc2*, confirming our previous results suggesting that this nucleic tool does not efficiently enter or transfect germ cells.

The method deployed here involved optimized, capped mRNA adapted for the expression of *Armc2*. The vector was injected via the rete testis into adult *Armc2* KO mice. The testes were then electroporated. The results obtained showed that the injected and electroporated testes had a morphology and weight similar to the controls at all times after treatment, thus validating the safety of the method in this preclinical model of male infertility.

Although motile sperm cells were observed at 3- and 5-weeks after *Armc2*-mRNA injection into the epidydimal cauda of *Armc2* KO mice, not all injected mice were efficiently treated. For instance, in a group of 5 mice littermates treated and euthanized at the same time (5 weeks post-injection), only 3 of the 5 had motile sperm cells. The absence of motile sperm at 5 weeks may be due to the type of spermatogenic cells transfected during the electroporation step. The transfected cells may differ between individuals, influenced by the injection and the position of the electrodes during electroporation. If the mRNA transfection takes place in a spermatogonia, it will take more than 6 weeks (including the time to cross the epididymis) before motile epididymal sperm cells emerge. This timeline could explain the absence of motile sperm in some littermates at 5 weeks.

Although we rescued the motility of oligo-astheno-teratozoospermic sperm, the transfection rate needs to be improved to obtain larger numbers of sperm cells. Indeed, our experiments did not provide enough motile sperm cells to carry out IVF or to allow natural mating. This

low proportion could be explained by the mode of cell transfection. Nevertheless, ICSI with normal sperm could be implemented, increasing the overall safety of the technique.

Naked mRNA, a new therapeutic strategy to treat severe infertility

Non-obstructive Azoospermia (NOA) and severe oligozoospermia (SO) are the most severe disorders of spermatogenesis and are the most likely to be of genetic origin. NOA is defined by the complete absence of spermatozoa in the ejaculate. Approximately 10–15% of infertile men have azoospermia, and a further 15% have SO [21]. For patients with NOA, few clinical solutions are currently available. Generally, testicular sperm extraction is attempted to collect some spermatozoa from the seminiferous tubules, which can then be used for ICSI [22]. When no sperm are retrieved, intra-conjugal conception is impossible. Our results could also be applied to treat NOA, even if synthesis of the target protein does not persist throughout the whole spermatogenesis cycle. Indeed, it has been shown that spermatogenic proteins have a very low turnover [23] because synthesized proteins are stored in sperm organelles which remain stable until fertilization. Consequently, fertility rescue can probably be achieved even for proteins expressed earlier and involved in meiosis. Moreover, the presence of a few sperm in the ejaculate could be sufficient to obtain pups because with ICSI, only one sperm is required per oocyte. In other words, the persistent expression is not mandatory to treat infertility.

We used in this report electroporation to transfect the testicular cells. Although we injected 2/3 of the testes, the transfection is limited by the size of the electrodes which produce a restricted electric field. To increase the testicular transfection rate, encapsulation of mRNA into lipids nanoparticles could be used, as used for Covid vaccination [24]. During the writing of this manuscript, Dong team [25], used a self-amplifying RNA (saRNA) encapsulated in cholesterol-amino-phosphate derived lipid nanoparticle to restore spermatogenesis in infertile mice. They successfully restore the expression of the DNA Meiotic Recombinase 1 (DMC1) in *Dmc1* KO infertile mice by injecting a self-amplifying RNA-*Dmc1* in the testes. Dmc1 is 37 KDa protein implicated in the meiotic recombination during sperm meiosis [26-28]. Although this impressive article reported successful treatment of mouse infertility, a safety study should be carried out to validate such a method. Indeed, saRNA are genetically engineered replicons derived from self-replicating single-stranded RNA viruses [29]. They can be delivered encapsulated in lipid nanoparticles, or as a completely synthetic saRNA

produced after the *in vitro* transcription. The saRNA contains the alphavirus replicase genes and encodes an RNA-dependent RNA polymerase (RdRP) complex which amplifies synthetic transcripts in situ and the target RNA sequence. The target RNA is expressed at high levels as a separate entity. As a result of their self-replicative activity, saRNAs can be delivered at lower concentrations than conventional mRNA to achieve comparable expression levels [30]. Moreover, saRNA constructs need to be condensed by a cationic carrier into a nanoparticle measuring ~100 nm to enable their uptake into target cells and protect the saRNA from degradation [31]. Finally, saRNA will amplify the RNA without cellular regulation. For all these reasons, if such a strategy is to be pursued, a potential toxicity effect due to saRNA over expression must be investigated in the testes and progeny. Another difficulty with saRNA relates to the size of the molecular construct. saRNA sequences are large and complex. The length of the sequence RdRP is around 7 kilobases, which often makes the full length of saRNA more than 9 kilobases once the sequence for the protein of interest has been integrated [31]. Dong et al. [25] successfully used their saRNA construct to rescue spermatogenesis failure induced by the absence of the small protein Dmc1, but it may be more challenging with larger proteins such as the structural proteins involved in OAT, including the 98-kDa ARMC2 [13].

Our next step will be to assess whether encapsulating *Armc2*-mRNA in LNP-CAP could allow a larger number of germ cells to be transfected.

In conclusion, this paper presents the first *in vivo* testicular injection and electroporation of capped and poly A tailed mRNA, demonstrating that it is an efficient strategy to transfect male germ cells and that the duration of expression of the resulting proteins is compatible with restoring spermatogenesis. Our comprehensive study revealed mRNA to be more efficient than an episomal vector, despite longer-lived expression in male germ cells with EEV. The difference was linked to EEV achieving a lower rate of seminiferous tubule transfection and a shorter duration of expression in germ cells. Our results also showed for the first time that functional sperm motility can be restored in mice with an oligo-astheno-teratozoospermia phenotype using a technique combining injection and electroporation of capped and poly-A-tailed mRNA. The findings presented open new opportunities to develop efficient strategies to treat male infertility with monogenic causes.

691

692 **Legends**

693 **Figure 1: Distribution of I-particles NIRFIP-180 in testis injected via the rete testis route.**

694 (A) A solution containing 0.05% Fast Green and 1% fluorescent i-particles NIRFiP-180 was
695 prepared, 10 µL was injected into the seminiferous tubules of adult males, through the *rete*
696 *testes* and its efferent channels. Injection was performed at constant pressure under a
697 binocular microscope. The progression of filling of the seminiferous tubules was monitored
698 thanks to the Fast Green (B). The testes were only filled to 2/3 capacity in order to prevent
699 damage to the tissue. (C) Representative distribution of fluorescent i-particles NIRFiP-180 in
700 a whole cross-section of an injected testis. Nuclei were counterstained with DAPI (blue
701 emission) to reveal tubules. (D) Enlargement of a seminiferous tubule showing particles
702 localized inside the lumens of the tubules. Scales bars: 1 mm and 500 µm.

703 **Figure 2: *In vivo* injection and electroporation do not alter the morphological structure of**
704 **the testes, seminiferous tubules, or sperm cells.**

705 (A, B) Testicular morphology was not affected by *in vivo* injection and electroporation of EEV-
706 *GFP* (A) or *GFP*-mRNA (B). Controls corresponds to contralateral testes
707 injected/electroporated with control solution (PBS, 0.05% FG). (A1, B1) comparison of the
708 testicular morphology of adult testes injected with nucleic acid vectors or control solutions.
709 (A2, B2) Comparison of testicular weight and (A3, B3) testicular length on day 7 after
710 injection/electroporation. Data are represented as a box plot median (n=4 for each
711 condition). A Wilcoxon matched pairs test was used to assess the significance of any
712 differences in testis weights and lengths, and p values of ≤0.05 were considered statistically
713 significant.

714 (C) Intact testicular structure after *in vivo* injection and electroporation with EEV-*GFP* and
715 *GFP*-mRNA. Comparison of testicular cross section structures. Testes paraffin sections were
716 stained with eosin/hematoxylin and observed by light microscopy (20X magnification). (C1)
717 Control, (C2) EEV-*GFP* injected and (C3) *GFP*-mRNA injected. Scales bars: 1000 µm.

718 (D) Seminiferous tubule structures are not affected by *in vivo* injection and electroporation
719 with EEV-*GFP* and *GFP*-mRNA. Enlargement of cross sections showing the fine structure of a

720 seminiferous tubule for control (D1), EEV-*GFP* (D2) and *GFP*-mRNA (D3). In each tubule the
721 different layers of spermatogenic cells are indicated, Sertoli cells (S), Spermatogonia (Sg),
722 Spermatocytes (Scytes), rounds Spermatids (Stids) and sperm cells (Spz), Leydig cells (L).
723 Scales bars: 500 and 20 µm.

724 (E) The area of seminiferous tubules is not affected by *in vivo* injection and electroporation
725 with EEV-*GFP* and *GFP*-mRNA. Comparison of the seminiferous tubule diameter after
726 injection of nucleic acid vectors or control solutions. Data are represented as a box plot
727 median. The areas of seminiferous tubules (μm^2) were measured for round cross sections
728 of $n > 35$ tubules per testis section (n= 5 testis sections per condition). Statistical significance
729 was verified using a Student *t*-test.

730 (F) Injection/electroporation do not impact epidydimal sperm cells. Representative sperm
731 observed by light microscopy on day 7 after injection/electroporation with Control solution,
732 EEV-*GFP*, or *GFP*-mRNA. Scale bars: 10 µm.

733 **Figure 3: Kinetics of EEV-GFP expression following *in vivo* injection/electroporation: whole**
734 **testicular expression**

735 (A1-H1) Whole-mount testes on days 0, 1 ,7, 14, 21, 28, 35 and 42 after *in vivo* injection/
736 electroporation with EEV-*GFP*. (A2-H2) Under fluorescence observation, GFP expression was
737 detectable in transfected testes from 12-week-old B6D2 mice. (C3-H3) Insets show the
738 absence of autofluorescence in non-transfected control testes. (4X magnification). The GFP
739 expression presented a punctiform pattern in seminiferous tubules and was detected from 1
740 day to 42 days. Scales bars: 1 mm and 100 µm.

741 **Figure 4: Kinetics of *GFP*-mRNA expression following *in vivo* injection/electroporation:**
742 **whole testicular expression**

743 (A1-F1) Whole-mount testes on days 0, 1 ,7, 14, 21, and 28 after *in vivo* injection/
744 electroporation with *GFP*-mRNA. (A2-F2) Under fluorescence observation, GFP expression
745 was detectable in transfected testes from 12-week-old B6D2 mice. (A3-F3) Insets show the
746 absence of autofluorescence in non-transfected control testes. (4X magnification). The GFP
747 expression presented a continuous pattern in seminiferous tubules and was detected from 1
748 day to 21

749 days. Scale bars: 1 mm and 100 µm.

750 (G) Comparison of number of injected mice exhibiting reporter gene expression. Mice
751 injected with *GFP*-mRNA exhibited GFP expression from day 1 to day 21. Mice injected with
752 EEV-GFP exhibited GFP expression from day 1 to 49 days. (for EEV-GFP n=11 on day 1; n=13
753 on day 2; n=10 on day 3; n=14 on day 7; n= 5 on day 10; n= 12 on day 15; n=11 on day 21;
754 n= 12 on day 28; n=15 on day 35; n=17 on day 42 and n=9 on day 49) ; (for *GFP*-mRNA n=3
755 on day 1; n=4 on day 3; n=15 on day 7; n= 21 on day 15; n=15 on day 21 and n= 5 on day
756 28).

757 **Figure 5: Kinetics of EEV and mRNA expression by *in vivo* bioluminescence imaging.**

758 (A) *In vivo* bioluminescence imaging quantification of luciferase expression over time
759 following injection/electroporation of EEV-*GFP-luc*. (A1): EEV-*GFP-Luc* was injected into the
760 testes and electroporated on day 0. Bioluminescence signal was quantified at several time
761 points. Results are expressed as the percentage of the maximal signal (mean ± SEM; n=5
762 mice up to D2; n=4 from D3 to D28; n=3 from D35 to D98 and n=3 from D105 to D119). (A2)
763 *In vivo* bioluminescence images of a representative mouse at several time points after
764 administering EEV-*GFP-LUC* or PBS, and ex vivo bioluminescence images of testes after 119
765 days.

766 (B) *In vivo* bioluminescence imaging quantification of luciferase expression over time induced
767 by injection/electroporation of *LUC*-mRNA**.** (B1) *LUC*-mRNA was injected into the testes and
768 electroporated on day 0. Bioluminescence signal was quantified in the whole testis at several
769 time points. Results are expressed as the percentage of the maximal signal (mean ± SEM; n =
770 5 mice). (B2): *In vivo* bioluminescence images of a representative mouse at several time
771 points after administering *LUC*-mRNA or PBS, and *ex vivo* bioluminescence images of caput,
772 testes, and cauda after 28 days.

773 (C) Decay over time of the number of mice expressing reporter genes. Mice were injected on
774 day 0 with *LUC*-mRNA or EEV-*GFP-LUC* and the number of mice showing bioluminescence in
775 the testis was counted at different time points, from day 1 to day 119. For EEV-GFP: n=13 at
776 D1; n=13 at D2; n=4 from D3 to D28; n=3 from D35 to D98 and n=3 from D105 to D119. For
777 mRNA-Luc: n = 5 mice for all time points.

Figure 6: Testicular and cellular *GFP*-mRNA expression measured on optically cleared testis after 3D image reconstructions from light sheet microscopy acquisitions. Testes were injected/electroporated with *GFP*-mRNA on day 0. On day 1, whole testes were fixed and subjected to optical clearing. (A) Testes were observed before and after optical clearing on a binocular microscope. The right image shows the transparency of the testis after complete clearing, revealing the blue mesh throughout the organ. (B) The internal structure of a cleared testis was 3D reconstructed after lightsheet microscopy image acquisition. The reconstruction was possible only for a half testis due to light penetration constraints. Two opposing faces of the same testis are presented, allowing the distribution of GFP fluorescence throughout the seminiferous tubules to be measured. Pink fluorescence corresponds to the autofluorescence of interstitial cells located around the seminiferous tubules. Scale bars A: 1 mm and B:500 µm.

Figure 7: Cellular expression of EEV-*GFP* following *in vivo* injection/ electroporation. Testes were injected/electroporated with EEV-*GFP* on day 0. On day 1 and on day 7, whole testes were fixed and subjected to optical clearing. Cleared tested were observed by fluorescence microscopy. (A1-A3) On day 1, transfected seminiferous tubules showed dotted green fluorescence at low magnification (X10/0.45). Nuclei were counterstained with DAPI (blue staining) to reveal the structure of the seminiferous tubules. At the cellular level, fluorescence was detectable (B1-B3) in germ cells including Spermatogonia (Sg), Spermatocytes (Scytes) and round Spermatids (RStides), as well as (C1-C3) in Sertoli cells (SC). (D1-D3) On day 7, the GFP signal was lower at low magnification (X10/0.45) and detectable (E1-E3) only in Sertoli cells (40x/1.15 WI) (n=3). E4 is an enlargement of the red square in E3, allowing the cell type to be identified. Scale bars: 100 µm, 15 µm and 3 µm.

Figure 8: Cellular expression of *GFP*-mRNA following *in vivo* injection/electroporation. Testes were injected/electroporated with *GFP*-mRNA on day 0. On day 1 and day 7, whole testes were fixed and subjected to optical clearing. Cleared testes were observed by fluorescence microscopy. (A1-A3) On day 1, transfected seminiferous tubules showed strong broad-ranging green fluorescence at low magnification (X10/0.45). Nuclei were counterstained with DAPI (blue staining) to reveal the structure of the seminiferous tubule. At the cellular level, fluorescence was detectable in germ cells (B1-B3) including

Spermatogonia (Sg), Spermatocytes (Scytes) and round Spermatids (RStides), Sperm cells (Spz) and Sertoli cells (SC). B4 is an enlargement of the red square in B3, allowing the cell types to be identified. (D1-D3) On day 7, the GFP signal remained strong at low magnification (X10/0.45) and (E1-E3) was still detectable in all germ cell types and Sertoli cells (40x/1.15 WI) (n=3). E4 is an enlargement of the red square in E3, showing that testicular sperm were also stained. Scale bars: 100 µm, 15 µm and 3 µm.

Figure 9: ARMC2 localization in dissociated testicular cells observed by immunofluorescence. Cells from WT and *Armc2* KO mice were stained with antibodies against ARMC2 (red signal) and tubulin (green signal). In WT mice, ARMC2 is located in the flagellum of spermatids. In KO mice, no ARMC2 signal (red fluorescence) was observed in any cells.

Figure 10: *In vivo* co-injection of *Armc2*-mRNA and *eGFP*-mRNA followed by electroporation do not affect testes morphology and weight. Adult WT mouse testes were injected with a solution containing *Armc2*-mRNA and *eGFP*-mRNA. After injection, the testes were electroporated and mice were euthanized two weeks later. (A): Whole testis under white and blue lights on a fluorescence microscope (A1): control testes not injected or electroporated (A2): testes injected with *Armc2*-mRNA and *eGFP*-mRNA. *eGFP*-mRNA was co-injected to validate the transfection efficiency. (B): Ratio of injected/electroporated testis weights to control testis weights at several time points post-injection (3-, 6-, 10-, 15-, 21-, 28- and 35-days post-surgery). n= 1 mouse per time.

Figure 11: Sperm motility is restored in *Armc2* KO mice at 21 and 35 days after injection and electroporation of *Armc2-* mRNA. Adult *Armc2* KO mouse testes were injected with a solution containing *Armc2*-mRNA. After injection, the testes were electroporated. At different times (3-, 6-, 10-, 15-, 21-, 28-, and 35-days *post*-injection), sperm were extracted from the cauda epididymis of the injected testis, and the sample was then examined with a CASA system to identify the percentage of motile spermatozoa. n= 2 for 15 days, n= 3 for 3, 6 and 21 days, n= 4 for 10 days, and n= 5 for 28 and 35 days.

B) Morphology of sperm cells in *Armc2* KO mice injected or not with *Armc2*-mRNA. (B1-2): microscopic observation of epididymal sperm cells from a mature WT mouse. (B3-4): epididymal sperm cells from a mature *Armc2* KO mouse 35 days after

839 injection/electroporation with *Armc2*-mRNA. (B5-6): epididymal sperm cells from a control
840 *Armc2* KO male. Normal sperm cells were observed in the injected condition with *Armc2*-
841 mRNA. (White arow) Scale bars:10 µm.

842 **Fig supp 1: Damaged tubules observed by optical microscopy following overstimulation**

843 Adult mouse testes were *in vivo* injected and over electroporated using 10 square electric
844 pulses to induce damage. (A) Control testis (no injection/electroporation). (B1-B2) Over
845 electroporated testes showing damaged tubules as pearly white striations. Scale bars: 1 mm.

846 **Fig supp 2: EEV and mRNA maps**

847 (A) EEV-plasmid map. The EEV-plasmid contains GFP, EVB ori, GFP, Luciferase, and EBNA
848 sequences under the control of the GAGs promotor. (B) The mCherry plasmid contains the
849 mCherry gene under the control of a T7 promotor. (C) The EEV-*Armc2* plasmid contains GFP,
850 oriP, EBNA and *Armc2* sequences under the control of the CMV and T7 promotors. (D)
851 *mcherry*-mRNA was synthetized as described in Material and Methods. It was validated by
852 agarose gel electrophoresis: Lane 1: DNA size marker ladder (100 bp), lane 2: capped
853 *mcherry*-mRNA (IVT product), lane 3: *mcherry*-mRNA after DNAse treatment. Capped and
854 poly A tailed *mcherry*-mRNA migrated to the expected size of 876 bp. (E) Validation of
855 *Armc2*-mRNA. HEK cells were transfected with *Armc2*-mRNA or EEV-*Armc2*. ARMC2 protein
856 was detected by Western blot with an anti-HA primary antibody. The expected size for the
857 ARMC2 protein is 98 kDa**.**

858 **Fig supp 3: Testicular expression of *mcherry*-mRNA following in vivo electroporation**

859 (A1, B1, C1, D1, E1 and F1) Whole-mount testes on days 0, 1, 7, 14, 21, 28 after *in vivo*
860 injection/ electroporation. (A2, B2, C2, D2, E2 and, F2) Using fluorescence microscopy,
861 transfected testes from 12-week-old B6D2 mice express red mCherry fluorescence. mCherry
862 was detected in a diffuse pattern throughout the seminiferous tubules from day 1 to day 15.
863 (A3, B3, C3, D3, E3 and F3) images showing the absence of autofluorescence in non-
864 transfected Control testes. (4X magnification). Scales bars: 1 mm and 100 µm.

865 **Fig supp 4: Cellular expression of *mcherry*-mRNA following in vivo injection/**
866 **electroporation.** Cross sections (20 µm) of mouse testes on day 1 (AB) and day 7 (CD) after in
867 vivo injection and electroporation with *mcherry*-mRNA, observed under fluorescence

microscopy. Red signals correspond to successfully transfected testicular tubular cells; nuclei were counterstained with DAPI (blue). At the cellular level, mCherry fluorescence was detectable in Sertoli cells (SC); Spermatogonia (SG); Spermatocytes (Scytes); round Spermatids (RStides), and Sperm cells (Spz); on day 1 and day 7 (Plan-Apochromat 63x/1,4 Oil, WD 190µm) (n=3). Scale bars: 10 µm and 5 mm.

Fig supp 5: Decay over time of the number of mice exhibiting reporter gene expression following injection/electroporation of the three different mRNAs.

Mice were injected on day 0 with *LUC*-mRNA, *GFP*-mRNA or *mcherry*-mRNA and the number of mice showing bioluminescence or fluorescence in the testis was counted at different time points. For *LUC*-mRNA n= 5 mice at each time point. For *mcherry*-mRNA n=3 on day 1; n=4 on day3; n=15 on day 7; n= 21 on day 15; n=15 on day 21; n= 5 on day 28; n=5 on day 35; and for *GFP*-mRNA n=3 on day 12; n=7 on day 2; n=7 on day 3; n=12 on day 7; n= 13 on day 15; n=10 on day 21 ; n= 9 on day 28; n=17 on day 35 and n=5 on day 42).

Videos 1 and 2: 3D-microscopic reconstructions of face 1 and 2 of a testis injected with *GFP*-mRNA.

Video 3: CASA recording of WT epidydimal sperm cells

Video 4: CASA recording of *Armc2* KO epidydimal sperm cells

Videos 5 and6: CASA recordings of epidydimal sperm cells from *Armc2* KO mice on day 21 and day 35, respectively, after injection/electroporation with *Armc2*-mRNA.

Acknowledgments

This work was supported by ANR-20-CE18-0007 grant to JE. This work was supported by the Fondation pour la Recherche Médicale, grant number « ECO202006011669 » to CV.

Bibliography

1. Boivin, J., et al., *International estimates of infertility prevalence and treatment-seeking: potential need and demand for infertility medical care*. Hum Reprod, 2007. **22**(6): p. 1506-12.
2. Thonneau, P. and A. Spira, *Prevalence of infertility: international data and problems of measurement*. Eur J Obstet Gynecol Reprod Biol, 1991. **38**(1): p. 43-52.
3. Uhlen, M., et al., *Transcriptomics resources of human tissues and organs*. Mol Syst Biol, 2016. **12**(4): p. 862.

4. Davies, M.J., et al., *Reproductive technologies and the risk of birth defects.* N Engl J Med, 2012. **366**(19): p. 1803-13.
5. Usmani, A., et al., *A non-surgical approach for male germ cell mediated gene transmission through transgenesis.* Sci Rep, 2013. **3**: p. 3430.
6. Raina, A., et al., *Testis mediated gene transfer: in vitro transfection in goat testis by electroporation.* Gene, 2015. **554**(1): p. 96-100.
7. Michaelis, M., A. Sobczak, and J.M. Weitzel, *In vivo microinjection and electroporation of mouse testis.* J Vis Exp, 2014(90).
8. Wang, L., et al., *Testis electroporation coupled with autophagy inhibitor to treat non-obstructive azoospermia.* Mol Ther Nucleic Acids, 2022. **30**: p. 451-464.
9. Sadelain, M., E.P. Papapetrou, and F.D. Bushman, *Safe harbours for the integration of new DNA in the human genome.* Nat Rev Cancer, 2011. **12**(1): p. 51-8.
10. Ishii, T., *Germ line genome editing in clinics: the approaches, objectives and global society.* Brief Funct Genomics, 2017. **16**(1): p. 46-56.
11. Duzgunes, N., J. Cheung, and K. Konopka, *Non-viral suicide gene therapy in cervical, oral and pharyngeal carcinoma cells with CMV- and EEV-plasmids.* J Gene Med, 2018. **20**(10-11): p. e3054.
12. Hodin, T.L., T. Najrana, and J.L. Yates, *Efficient replication of Epstein-Barr virus-derived plasmids requires tethering by EBNA1 to host chromosomes.* J Virol, 2013. **87**(23): p. 13020-8.
13. Coutton, C., et al., *Bi-allelic Mutations in ARMC2 Lead to Severe Astheno-Teratozoospermia Due to Sperm Flagellum Malformations in Humans and Mice.* Am J Hum Genet, 2019. **104**(2): p. 331-340.
14. in *Transforming and Scaling Up Health Professionals' Education and Training: World Health Organization Guidelines 2013*. 2013: Geneva.
15. Ruthig, V.A. and D.J. Lamb, *Updates in Sertoli Cell-Mediated Signaling During Spermatogenesis and Advances in Restoring Sertoli Cell Function.* Front Endocrinol (Lausanne), 2022. **13**: p. 897196.
16. de Boer, P., M. de Vries, and L. Ramos, *A mutation study of sperm head shape and motility in the mouse: lessons for the clinic.* Andrology, 2015. **3**(2): p. 174-202.
17. Ibtisham, F., et al., *Progress and future prospect of in vitro spermatogenesis.* Oncotarget, 2017. **8**(39): p. 66709-66727.
18. Lechtreck, K.F., et al., *Chlamydomonas ARMC2/PF27 is an obligate cargo adapter for intraflagellar transport of radial spokes.* Elife, 2022. **11**.
19. Kubo, T., et al., *Together, the IFT81 and IFT74 N-termini form the main module for intraflagellar transport of tubulin.* J Cell Sci, 2016. **129**(10): p. 2106-19.
20. Dai, J., et al., *In vivo analysis of outer arm dynein transport reveals cargo-specific intraflagellar transport properties.* Mol Biol Cell, 2018. **29**(21): p. 2553-2565.
21. Cocuzza, M., C. Alvarenga, and R. Pagani, *The epidemiology and etiology of azoospermia.* Clinics (Sao Paulo), 2013. **68 Suppl 1**: p. 15-26.
22. Ma, Y., et al., *A risk prediction model of sperm retrieval failure with fine needle aspiration in males with non-obstructive azoospermia.* Hum Reprod, 2019. **34**(2): p. 200-208.
23. Hermann, B.P., et al., *The Mammalian Spermatogenesis Single-Cell Transcriptome, from Spermatogonial Stem Cells to Spermatids.* Cell Rep, 2018. **25**(6): p. 1650-1667 e8.
24. Schoenmaker, L., et al., mRNA-*lipid nanoparticle COVID-19 vaccines: Structure and stability.* Int J Pharm, 2021. **601**: p. 120586.
25. Du, S., et al., *Cholesterol-Amino-Phosphate (CAP) Derived Lipid Nanoparticles for Delivery of Self-Amplifying RNA and Restoration of Spermatogenesis in Infertile Mice.* Adv Sci (Weinh), 2023. **10**(11): p. e2300188.
26. Takemoto, K., et al., *Meiosis-Specific C19orf57/4930432K21Rik/BRME1 Modulates Localization of RAD51 and DMC1 to DSBs in Mouse Meiotic Recombination.* Cell Rep, 2020. **31**(8): p. 107686.

27. Habu, T., et al., *The mouse and human homologs of DMC1, the yeast meiosis-specific homologous recombination gene, have a common unique form of exon-skipped transcript in meiosis.* Nucleic Acids Res, 1996. **24**(3): p. 470-7.
28. Shinohara, A., et al., *Saccharomyces cerevisiae recA homologues RAD51 and DMC1 have both distinct and overlapping roles in meiotic recombination.* Genes Cells, 1997. **2**(10): p. 615-29.
29. Tews, B.A. and G. Meyers, *Self-Replicating RNA.* Methods Mol Biol, 2017. **1499**: p. 15-35.
30. Bloom, K., F. van den Berg, and P. Arbuthnot, *Self-amplifying RNA vaccines for infectious diseases.* Gene Ther, 2021. **28**(3-4): p. 117-129.
31. Kim, J., et al., *Self-assembled* mRNA *vaccines.* Adv Drug Deliv Rev, 2021. **170**: p. 83-112.

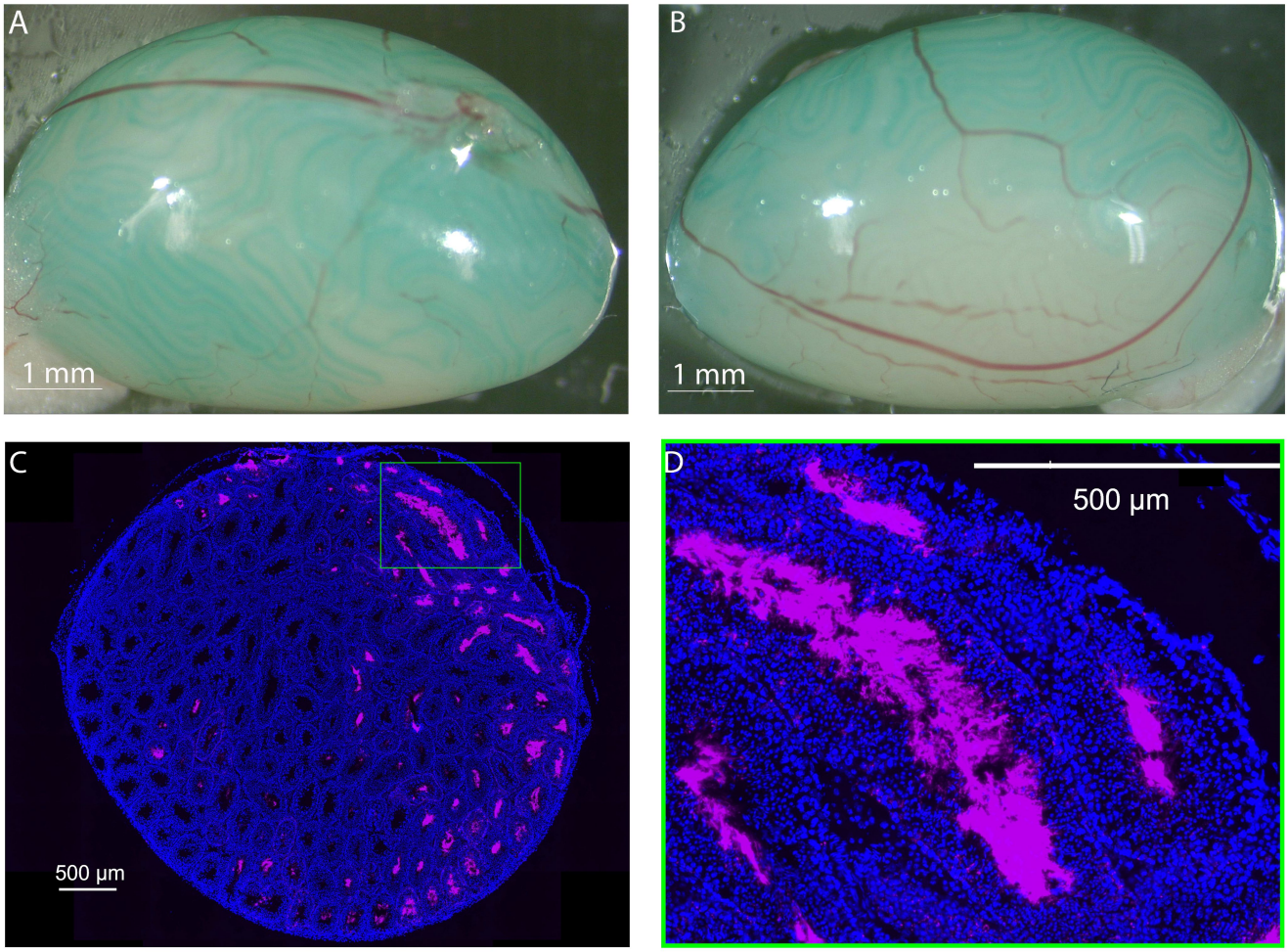

Figure 1, Vilpreux et al 2023

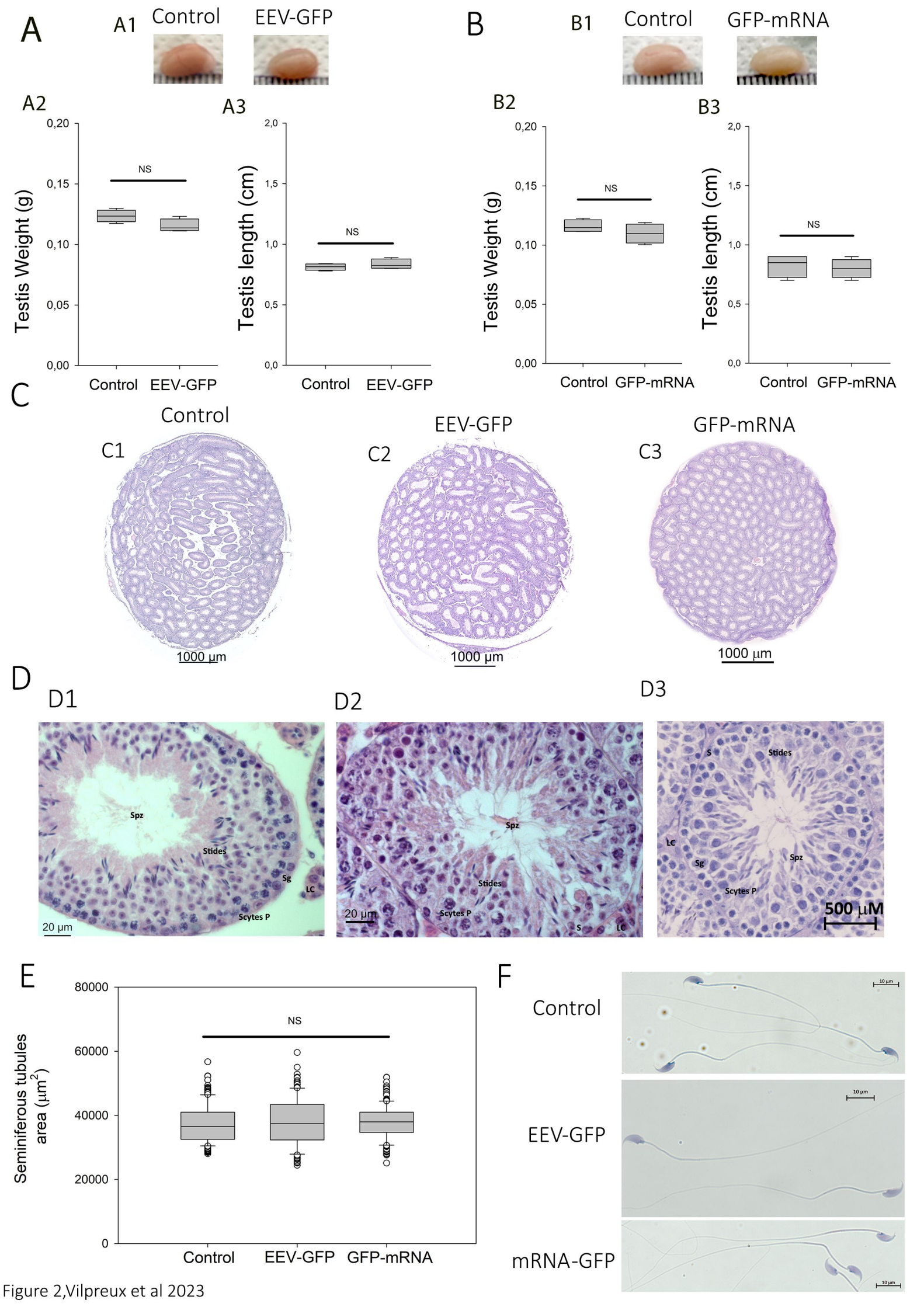

Figure 2,Vilpreux et al 2023

EEV-GFP

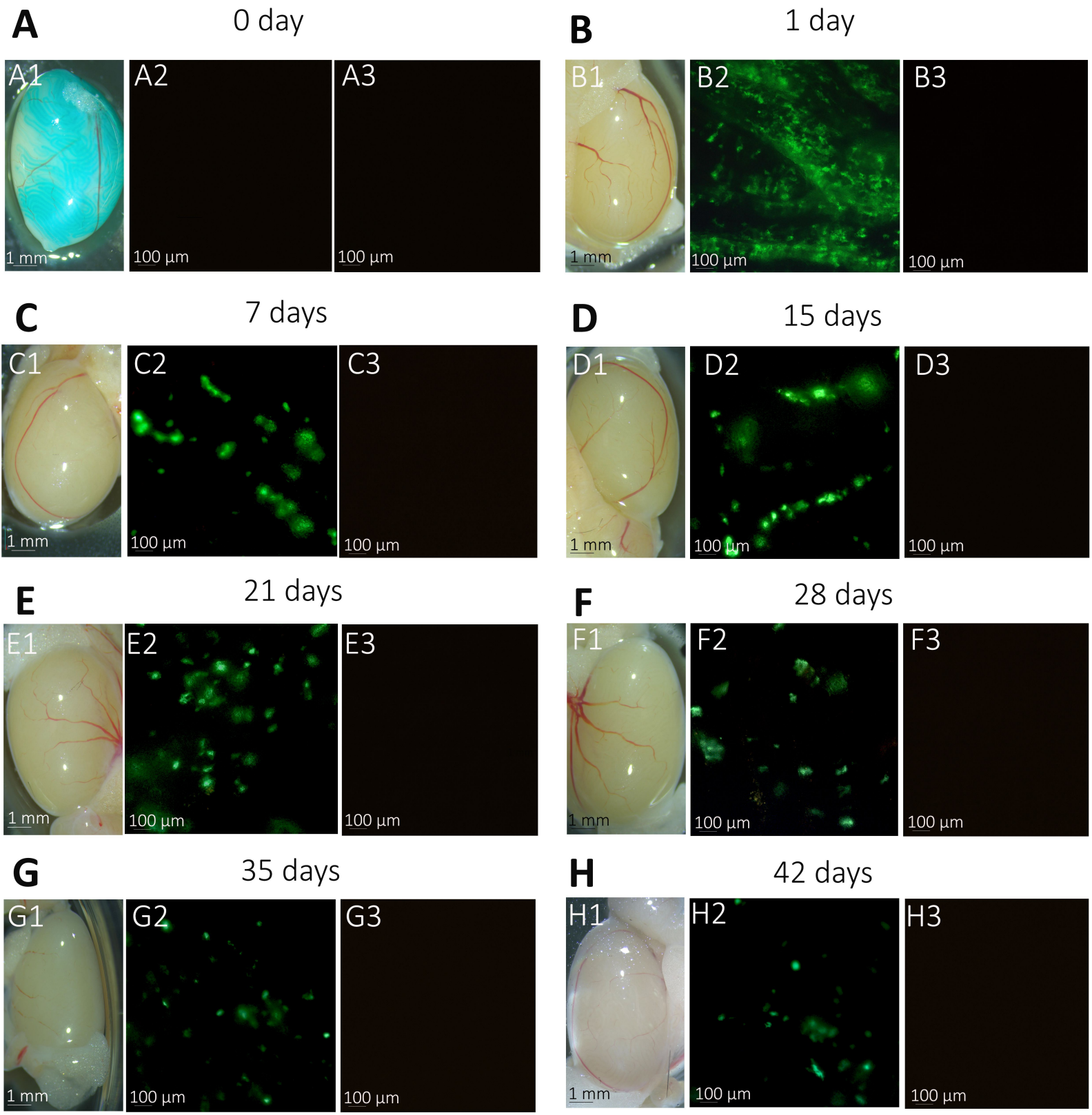

Figure 3,Vilpreux et al 2023

GFP-mRNA

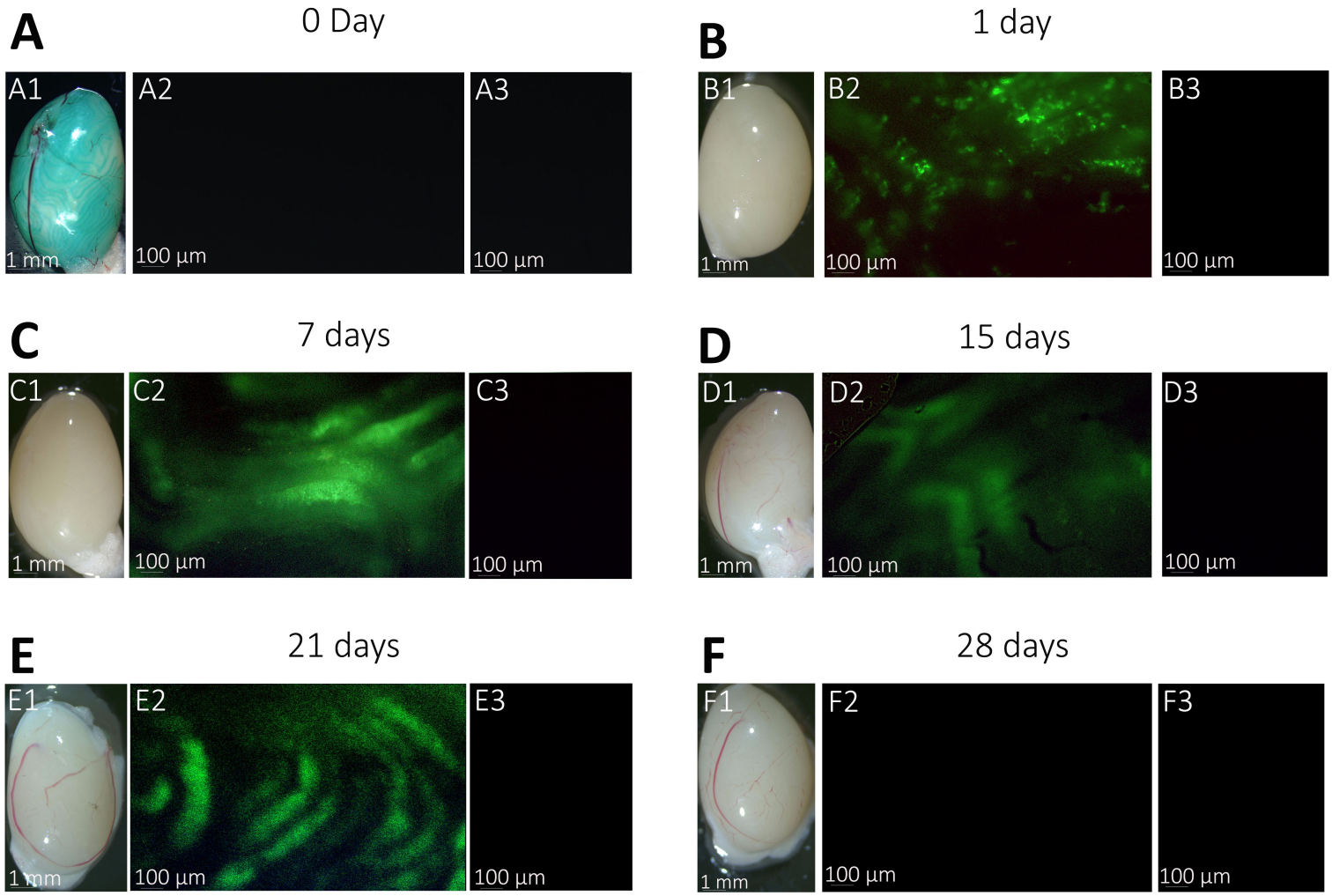

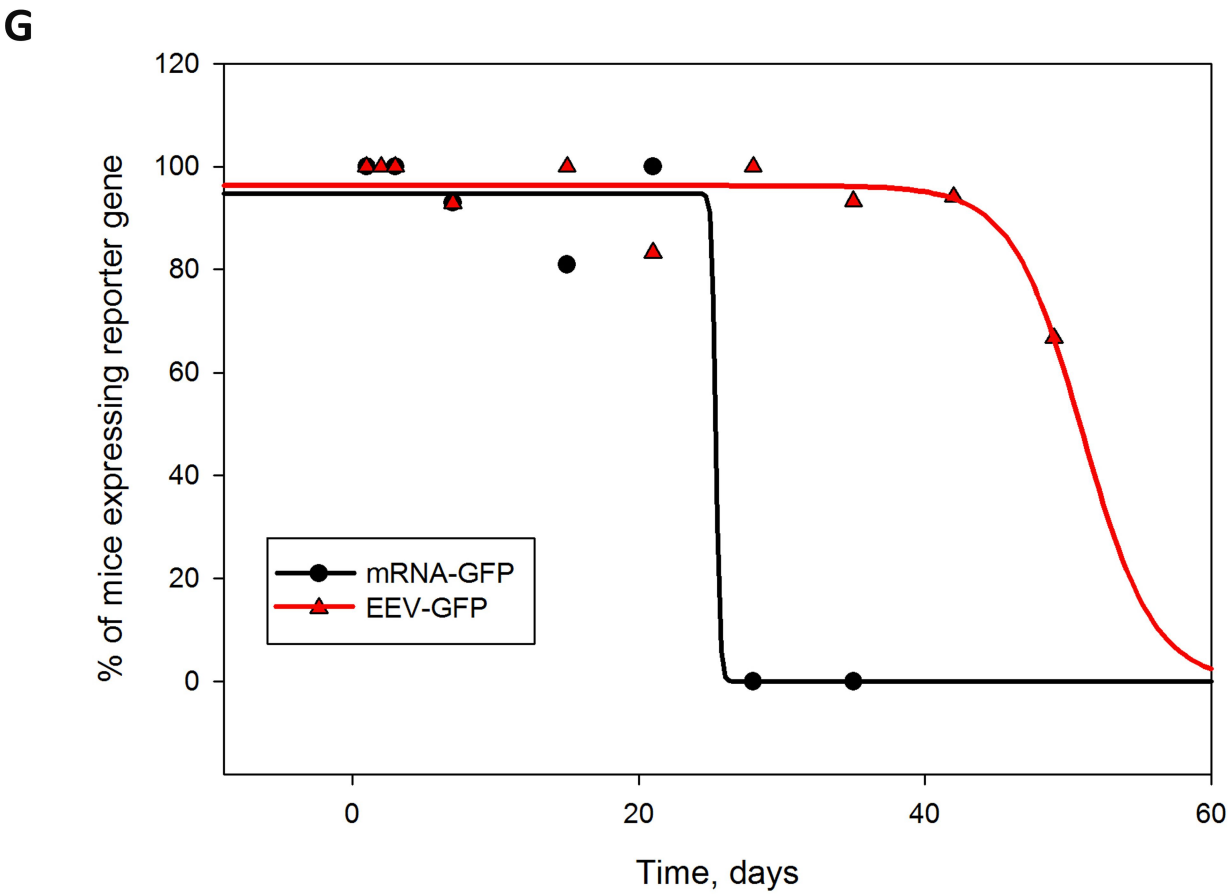

Fig4, Vilpreux et al 2023

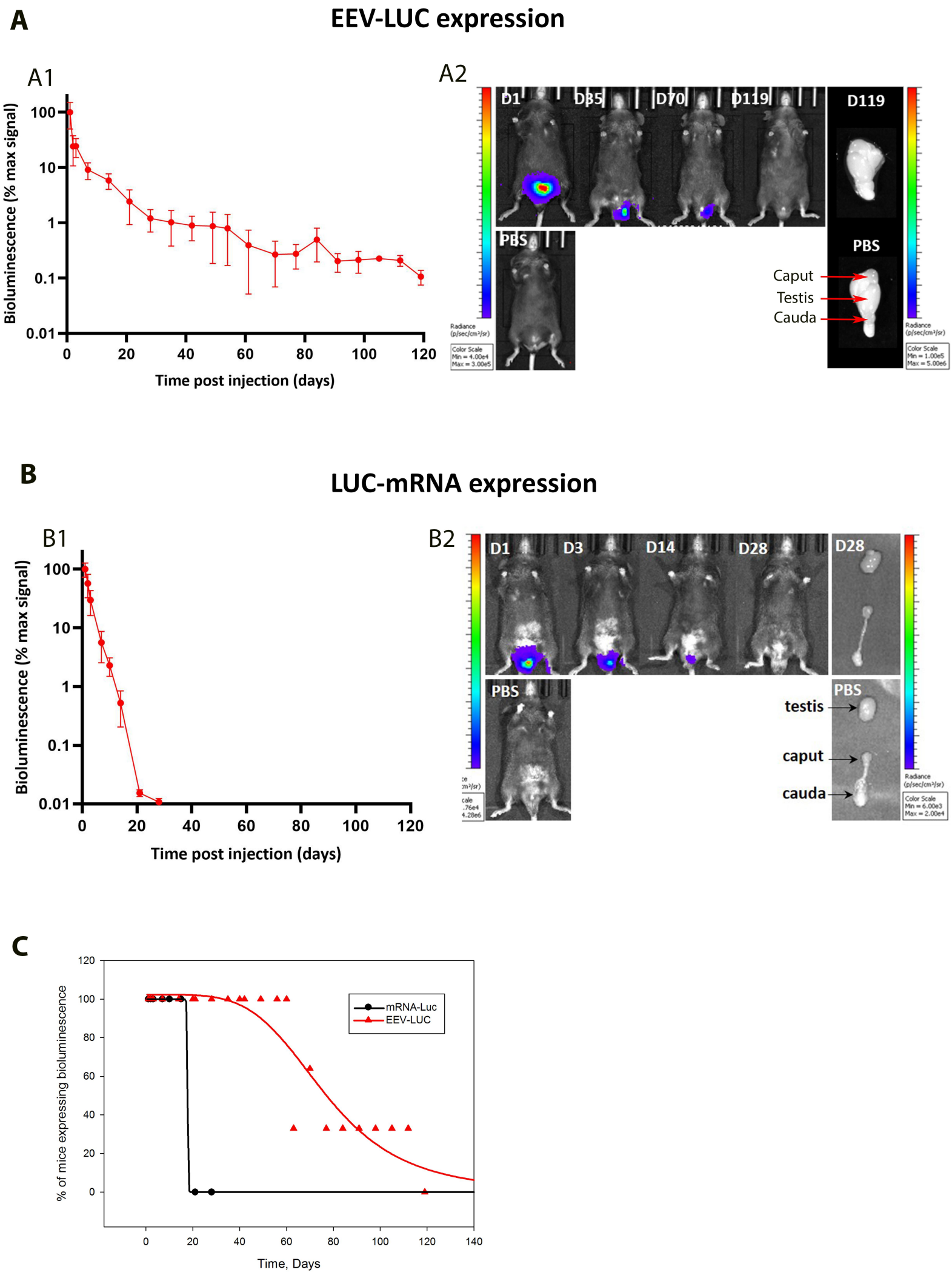

Figure 5, Vilpreux et al 2023

GFP-mRNA 1 day post injection

A

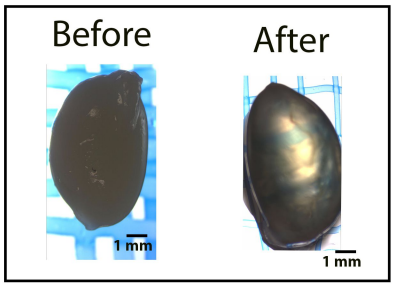

B

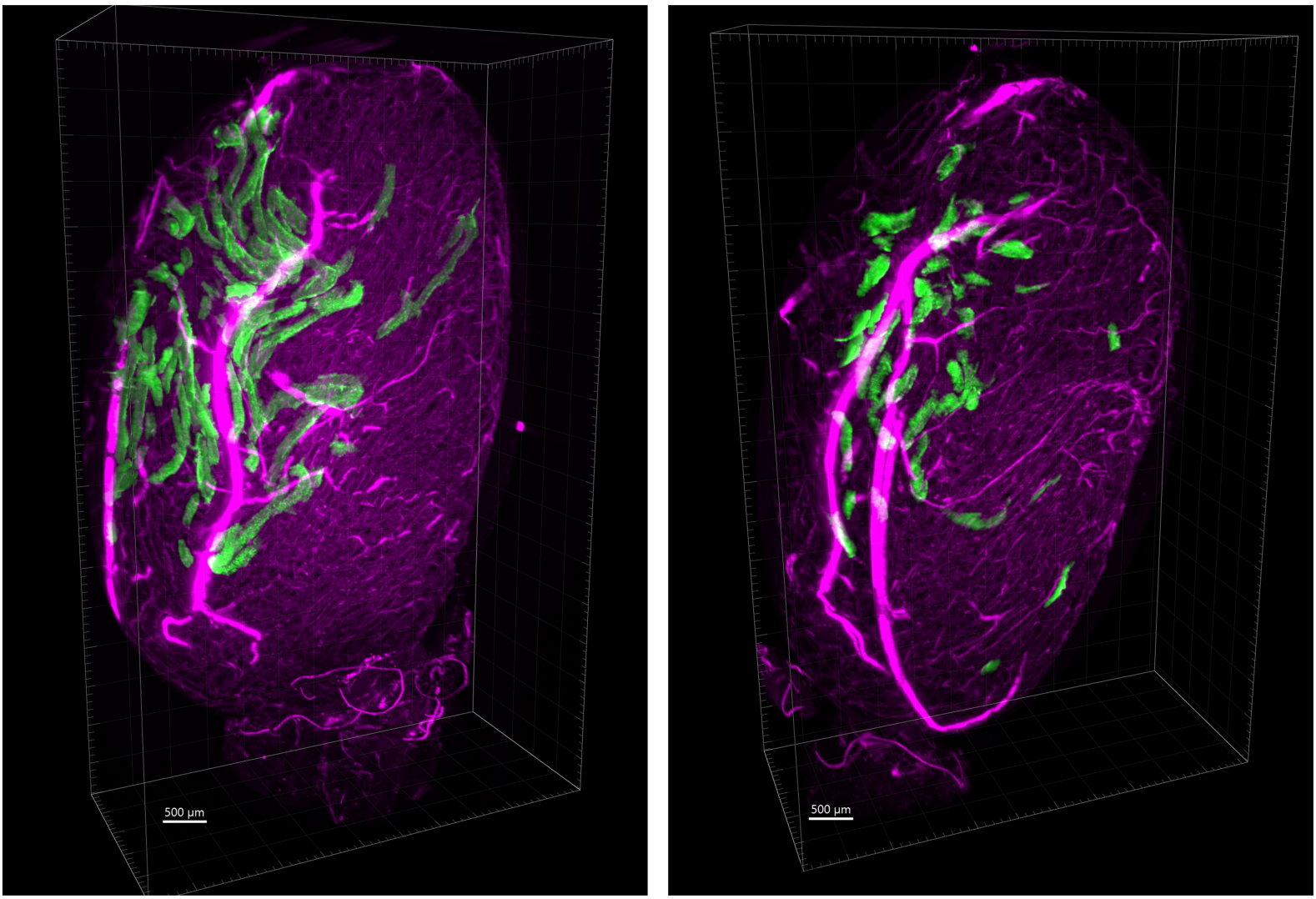

Figure 6, Vilpreux et al 2023

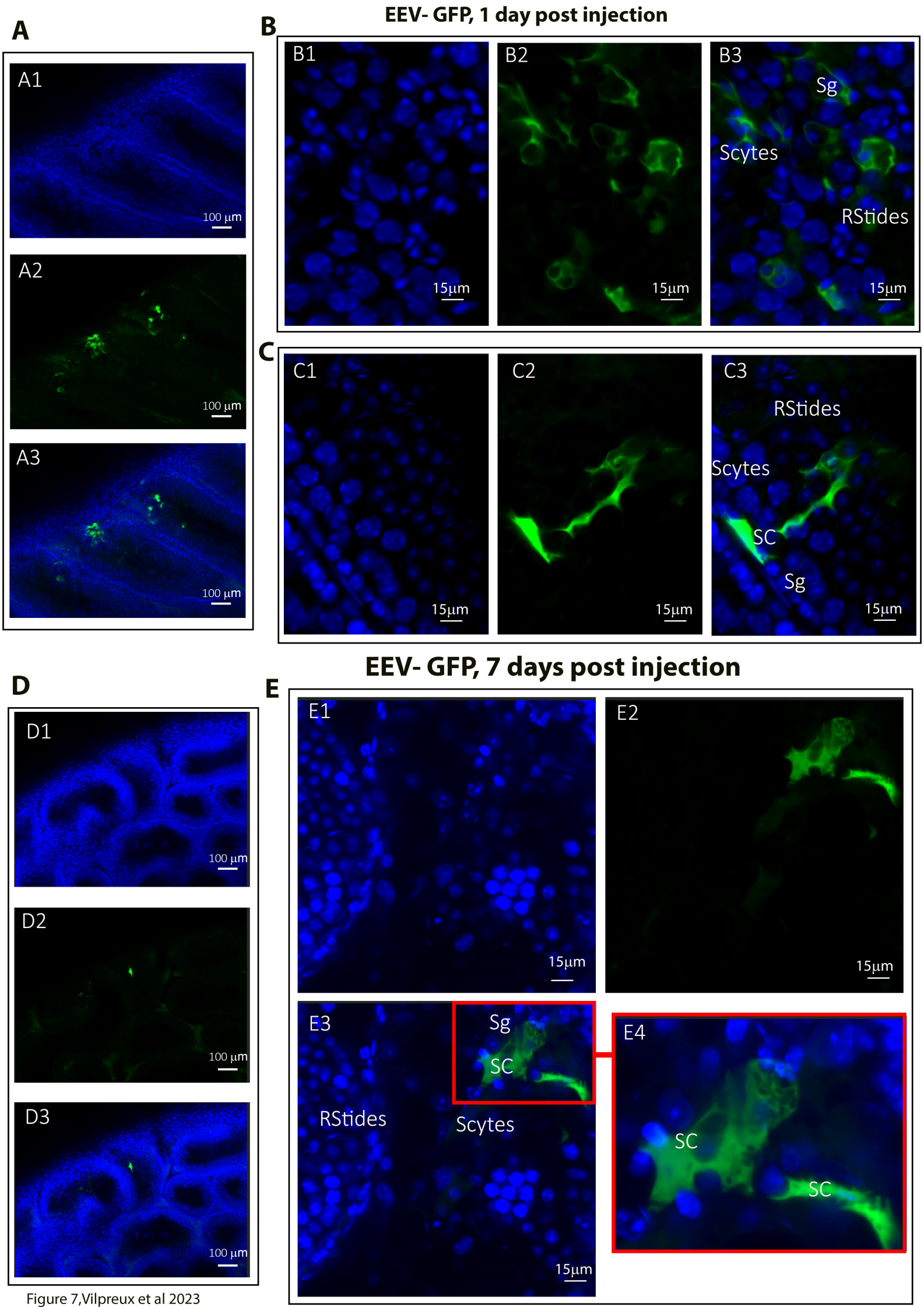

Figure 7,Vilpreux et al 2023

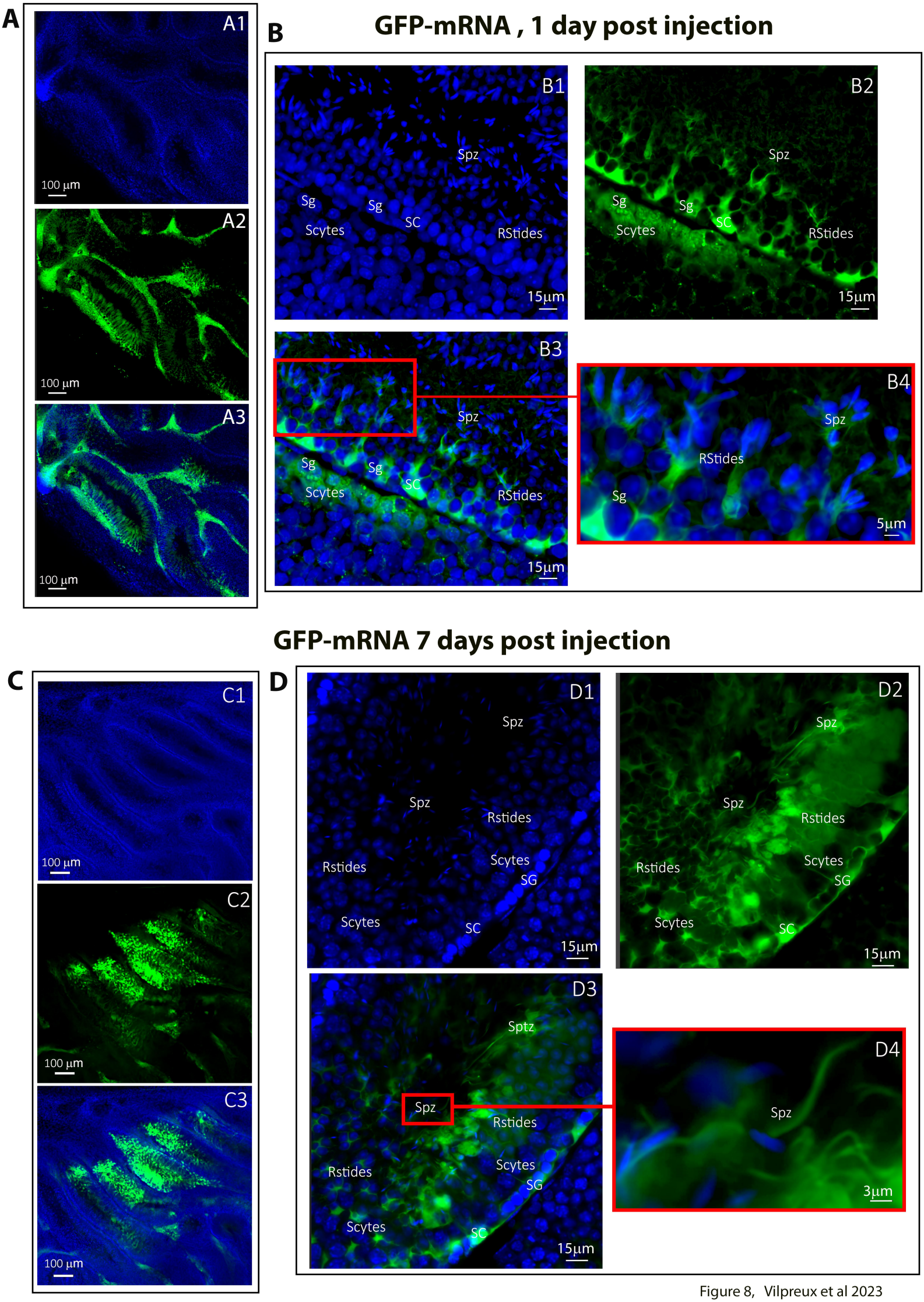

Figure 8, Vilpreux et al 2023

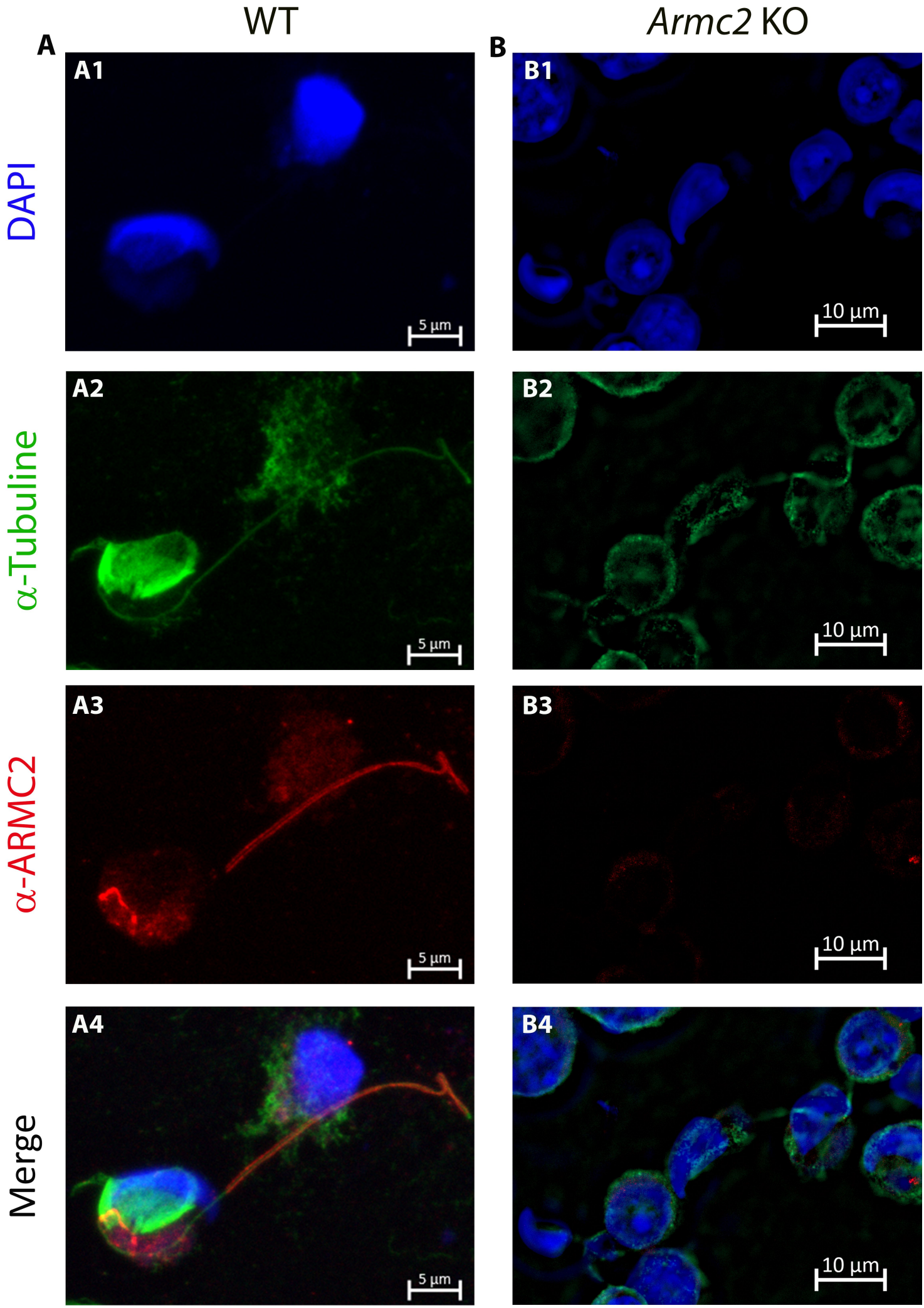

Figure 9, Vilpreux et al 2023

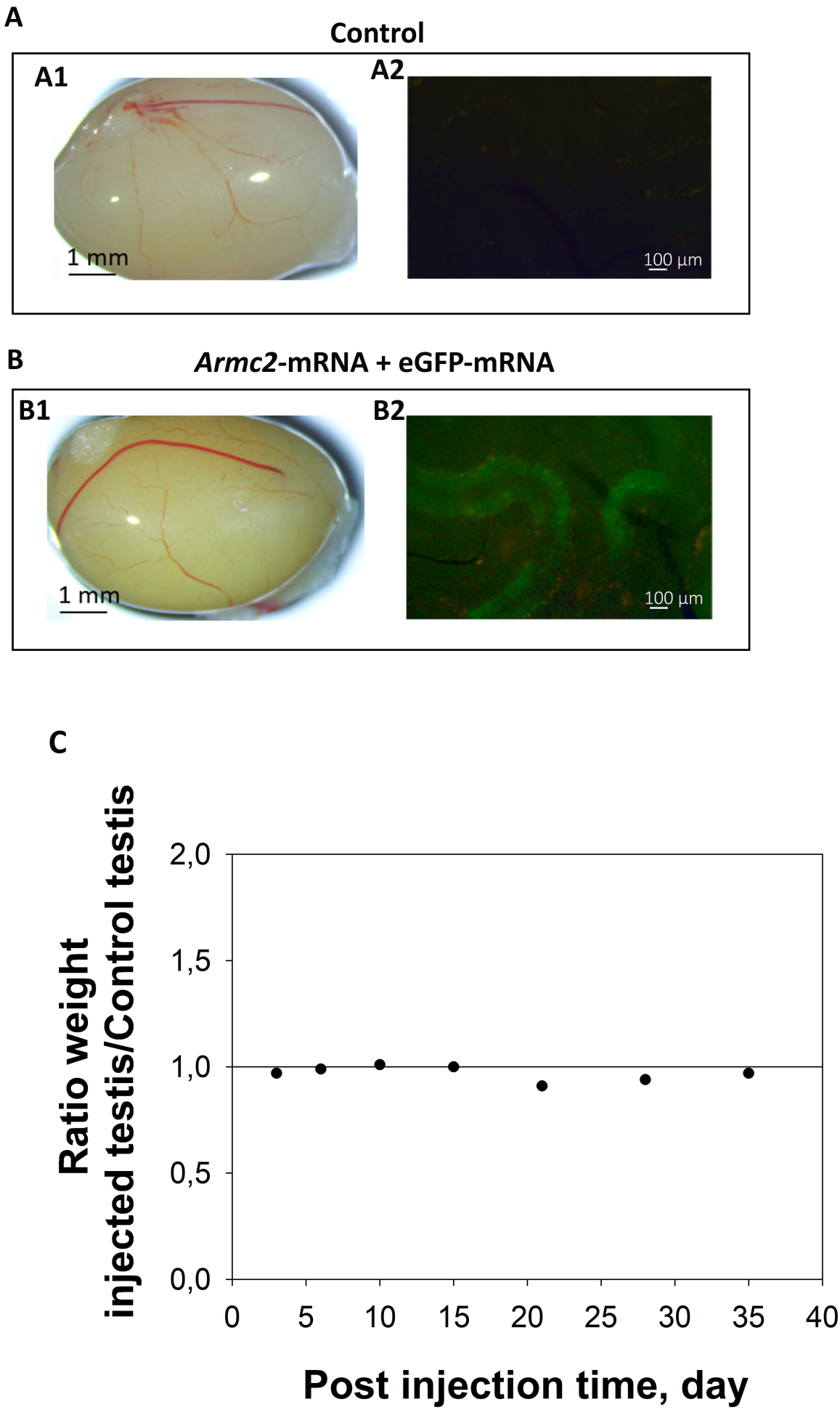

Figure 10, Vilpreux et al 2023

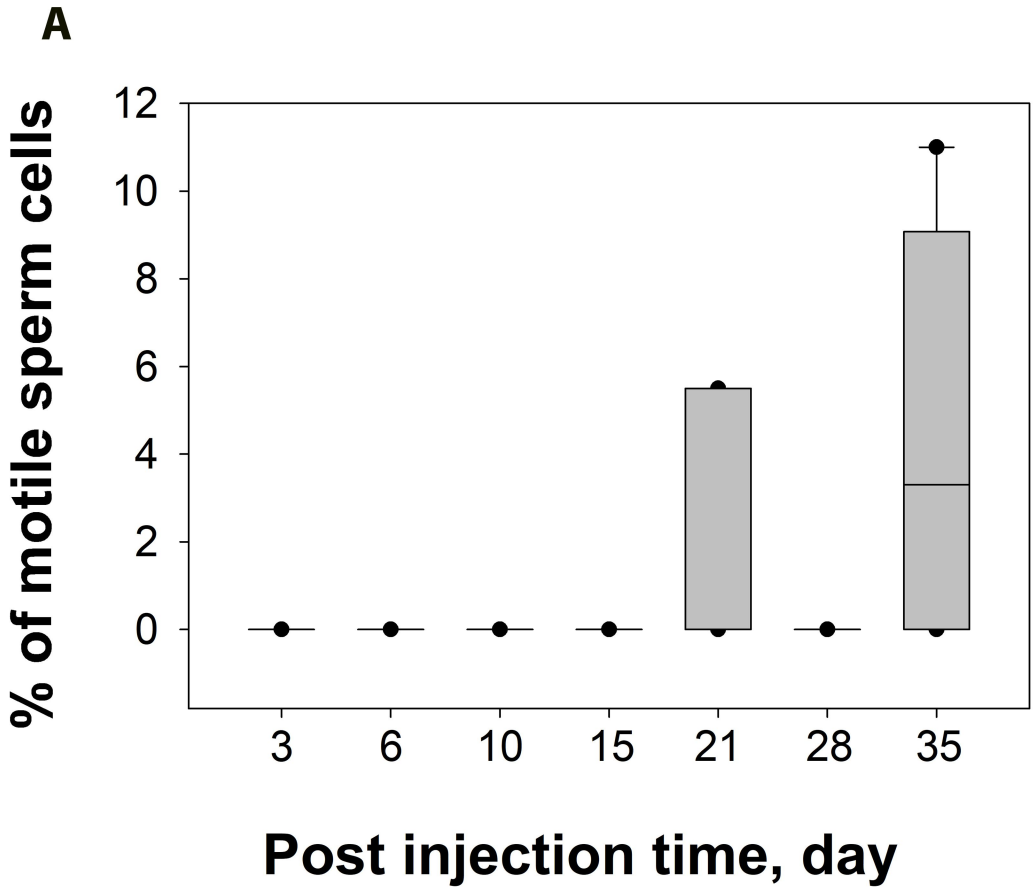

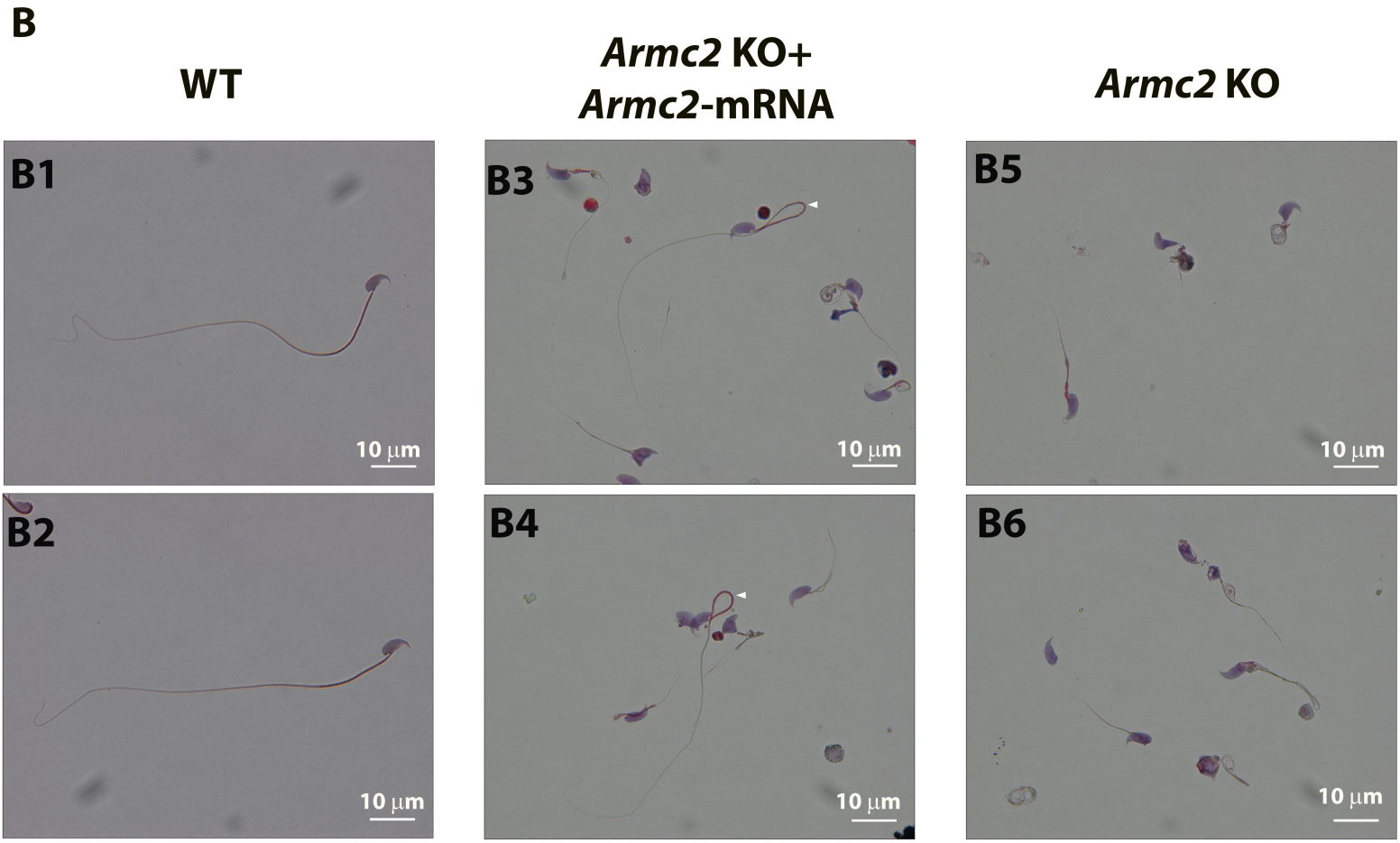

Figure 11,Vilpreux et al 2023

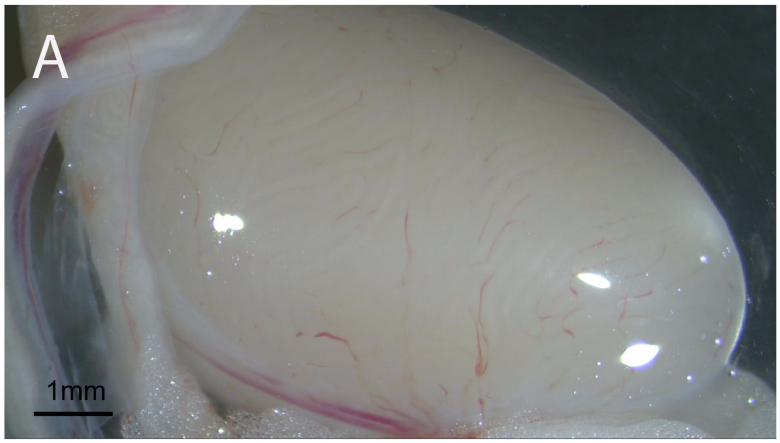

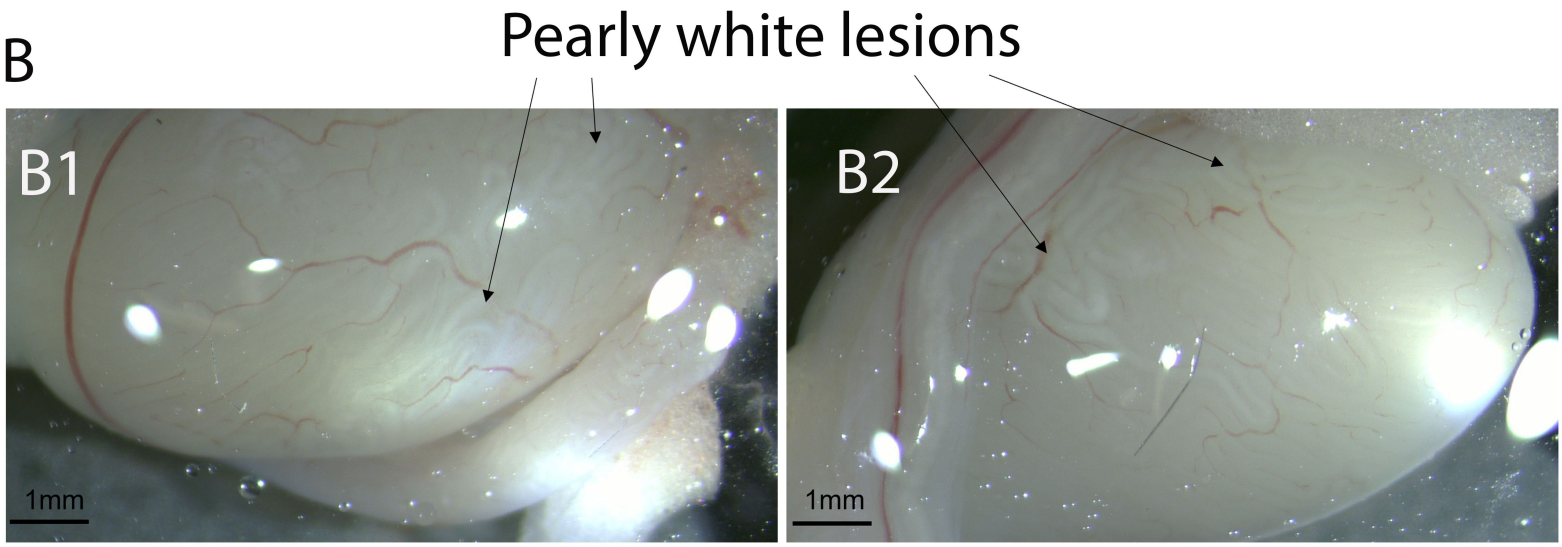

Figure supp 1, Vilpreux et al 2023

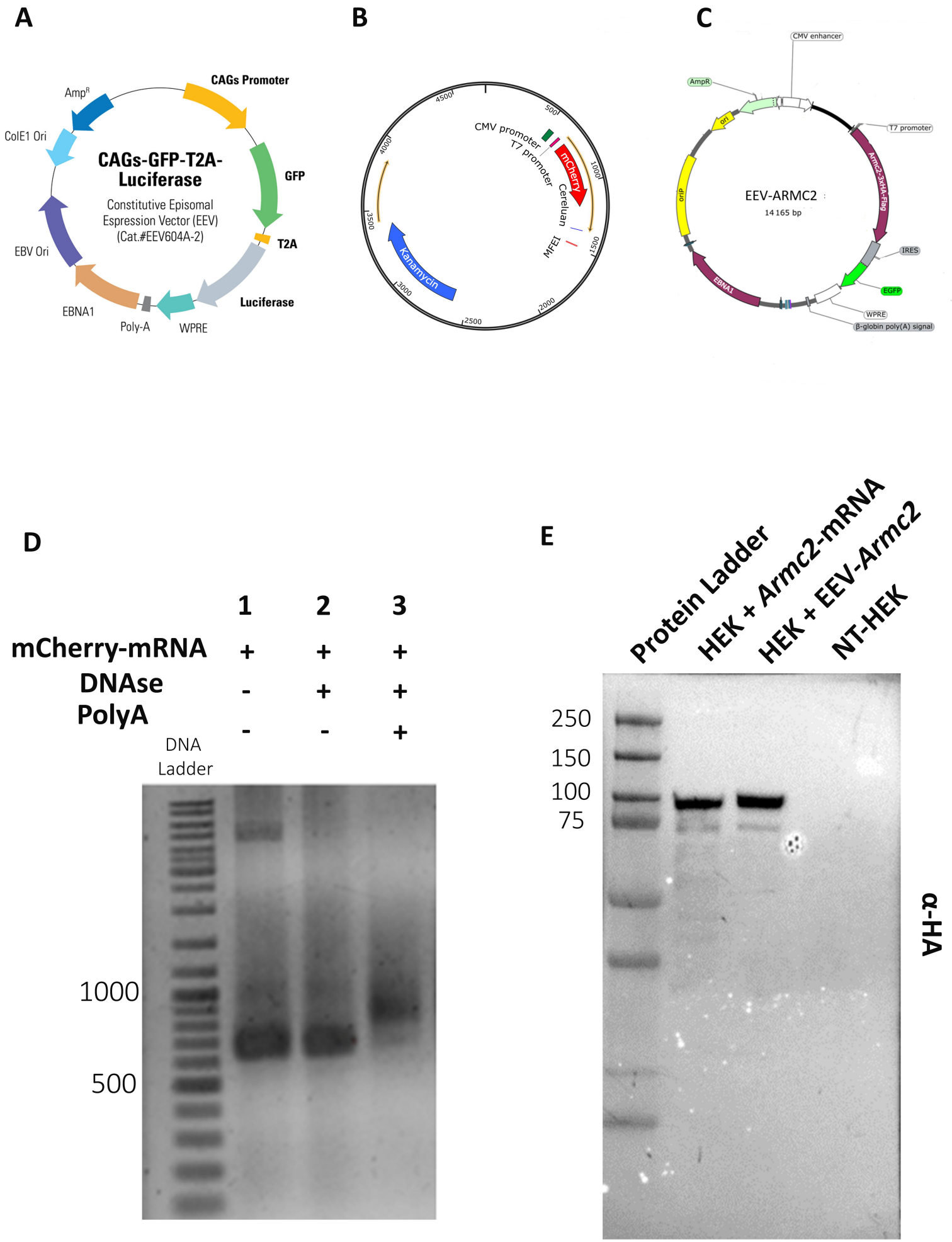

Fig supp2 ,Vilpreux et al 2023

mCherry-mRNA

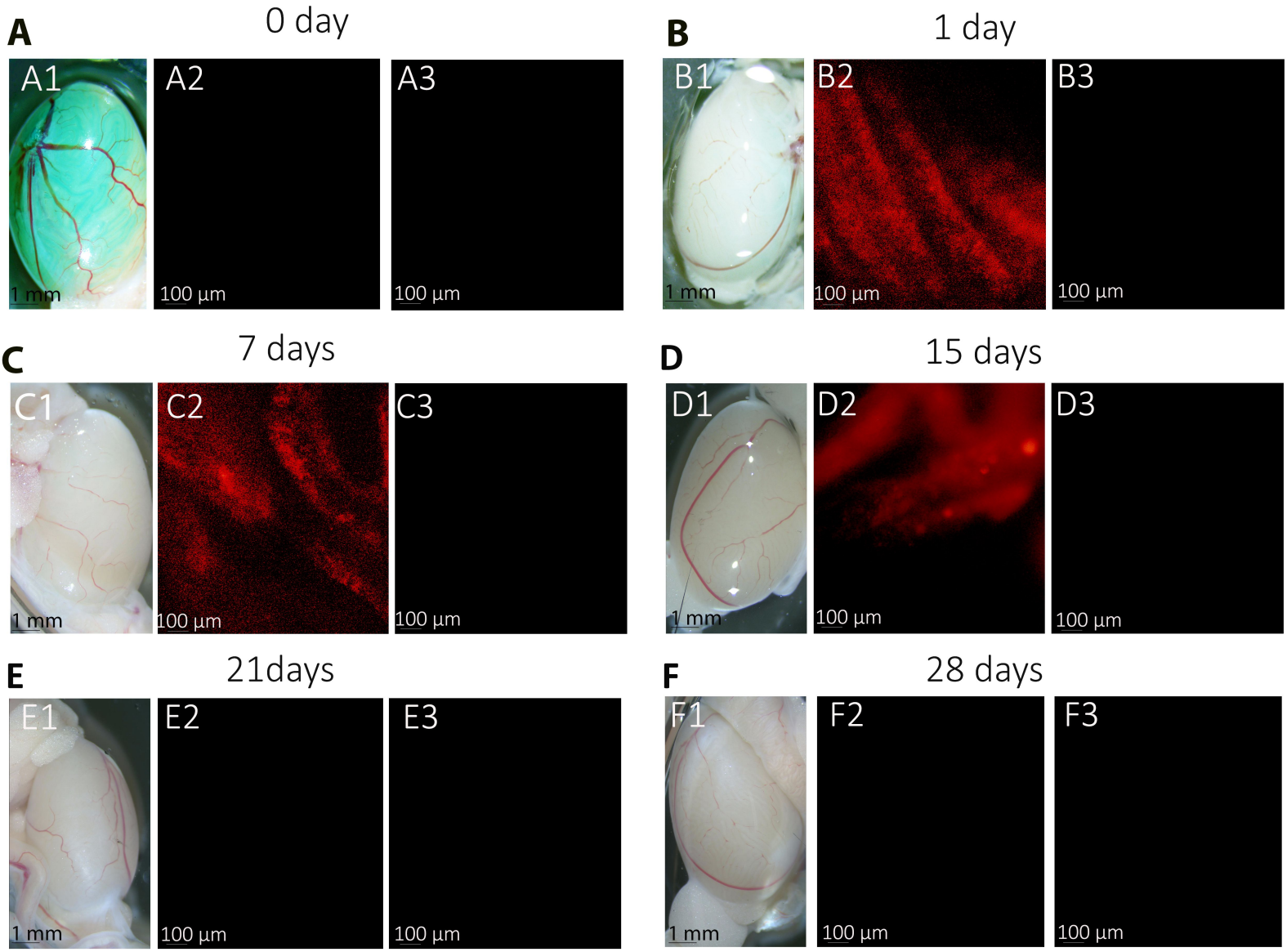

Figure supp 3 Vilpreux et al 2023

mCherry-mRNA , 1 day post injection

A

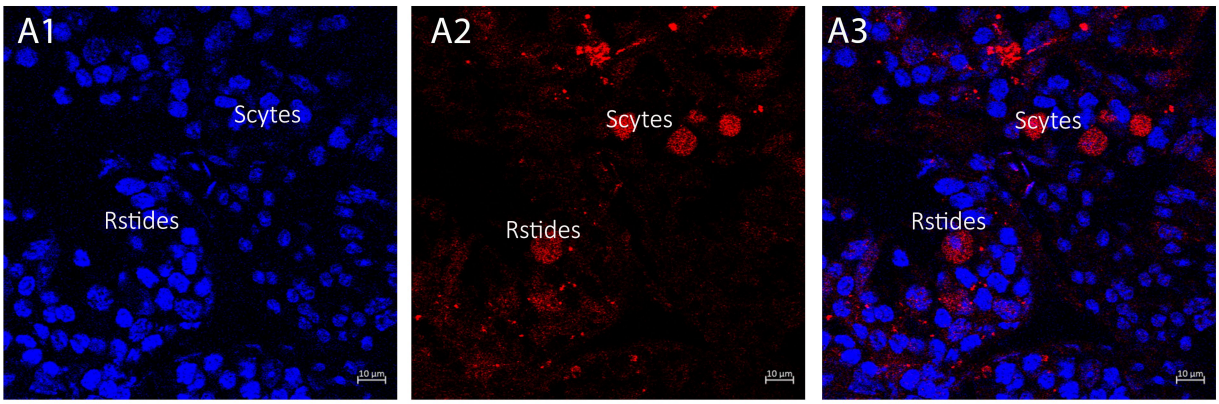

B

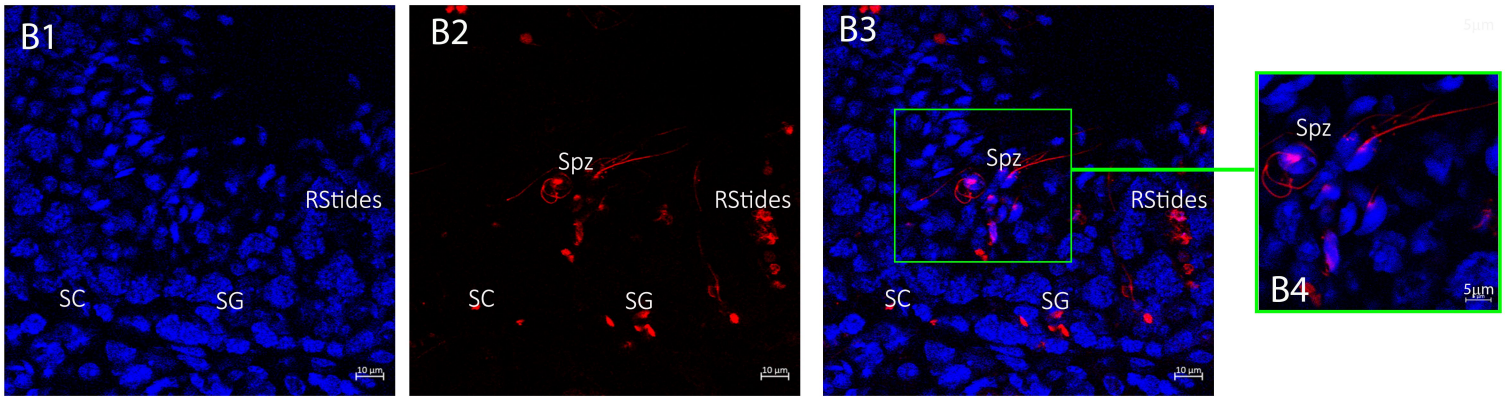

mCherry-mRNA, 7 days post injection

C

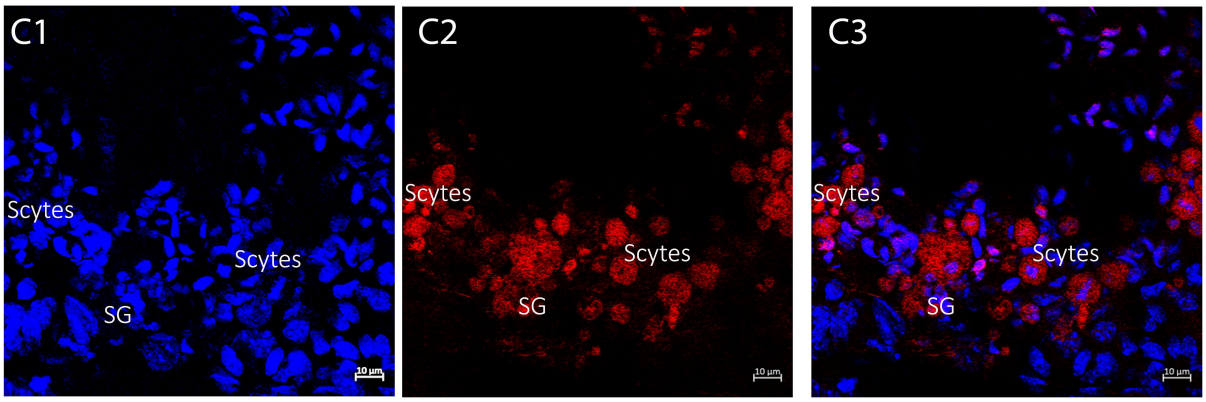

D

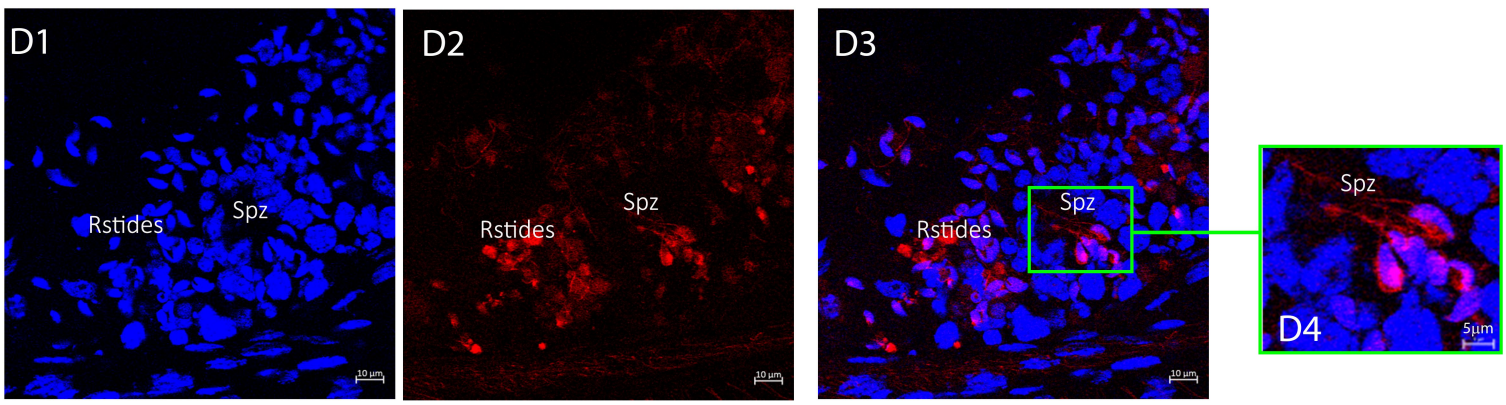

Figure supp 4, Vilpreux et al 2023

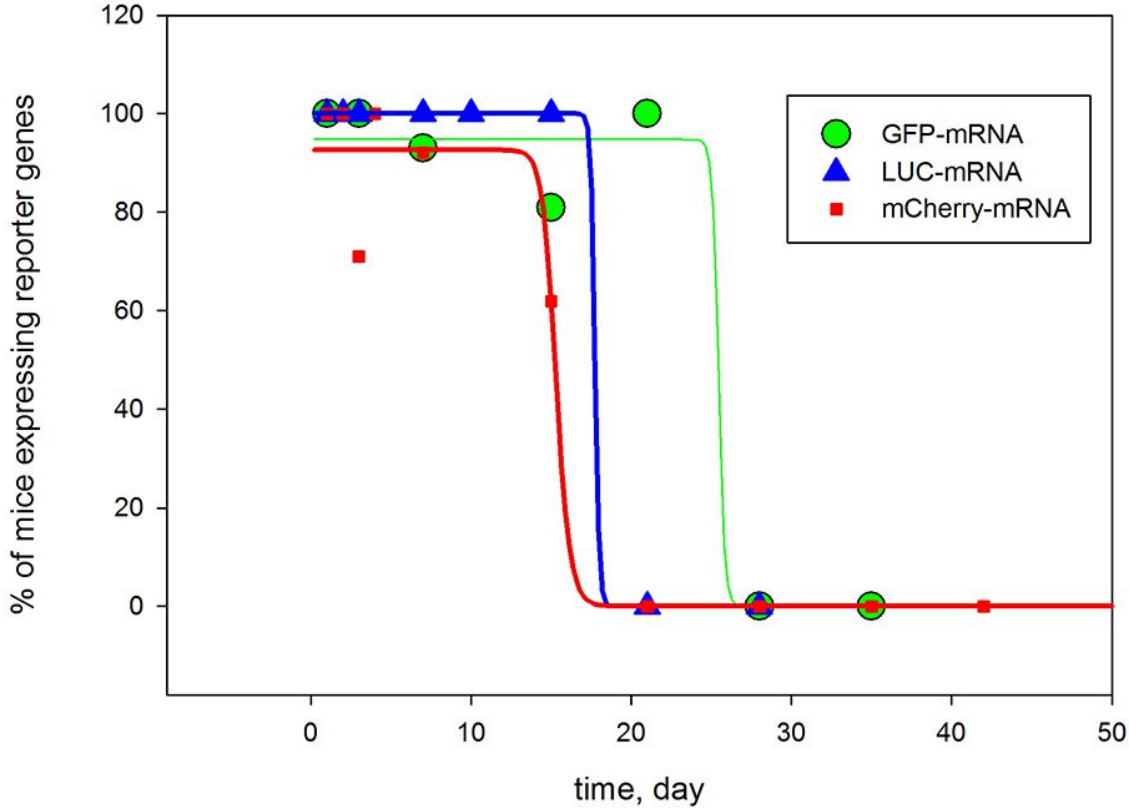

Figure supp 5, Vilpreux et al 2023